Πανεπιστήμιο Κύπρου
University of Cyprus

NUMERICAL MODELLING OF PRESTRESSED COLD-FORMED STEEL BEAMS WITH BOTTOM FLANGE OPENINGS

by

Anna Kaiki

A thesis submitted to University of Cyprus for the Master of Science in Earthquake Engineering

Department of Civil and Environmental Engineering

University of Cyprus

Nicosia, Cyprus

May 2024

Assurance of Originality

This Master thesis is a record of my own original study. Any information from other sources is recognized by properly citing the published or unpublished sources.

This thesis is being submitted to University of Cyprus for the Master of Science degree; it has not been submitted to another university for a degree or any other qualification.

Abstract

In the present thesis, the concept of using the prestressing method to improve the load-carrying capacity of cold-formed steel beams is presented. The prestressing is conducted using high-strength steel cables that are housed through openings in the bottom flange of the steel beams. Their prestressing delays the occurrence of instability phenomena and thus increases the strength of the cold-formed steel beams. This is due to the fact that the initial stresses generated by the prestressing have opposite signs to the stresses generated in the next stage of distributed loading. The total vertical deformation of the beam is significantly reduced due to the pre-camber induced along the beam during the prestressing stage and the contribution of the cable to the flexural stiffness of the system.

Prestressed cold-formed steel beams can provide efficient structural solutions since a smaller cross-section is required for a given demand in load-carrying capacity which enables a lighter solution for a given span and load. This thesis presents a conceptual approach to prestressed cold-formed steel beams with bottom flange openings. The mechanical behavior of the proposed structural system was studied using analytical and numerical models. The behavior of the proposed beam throughout the prestressing phase and the applied vertical load is simulated using finite element model.

Contents

Chapter 1 – Introduction

1.1 Initial Concept

Cold-formed steel (CFS) members have traditionally been used as load-bearing members in various applications, such as beams in roofing systems and construction coverings. In recent years, CFS panels have become increasingly popular in high-rise, low and mid-rise buildings, as well as CFS gate frames with small to medium openings.

CFS sections are increasingly being used and offered as an alternative to hot-formed steel elements. This is due to the fact that there is more flexibility in terms of profiles and section sizes, less material is wasted, which can lead to more cost-effective design solutions. They are also stronger, lighter in weight and easier to manufacture than hot-formed components (GJ Hancock, 2016; Schafer, 2017). However, the thin geometry of CFS components makes them vulnerable to local, distortional, and global buckling. It is therefore essential to predict and avoid these instability phenomena. The instability phenomena are likely to occur at stresses below the yield point of the material, leaving the capacity of the cross-section completely untapped. These phenomena can be significantly delayed by prestressing, as recently reported by Hadjipantelis, et al. (2018).

In general, prestressing techniques are often used to increase the load-bearing capacity and functionality of components and systems. It is usually widely used for concrete structures, but the advantages it can offer for steel structures are equally important, as first suggested by G. Magnel, (1950). The application of prestressing to steel elements aims to improve the performance of the element by applying stress at points prone to instability, resulting in specific stresses within the element under load. It partially or fully cancels the stresses that occur in the area. In concrete structures, the purpose of prestressing is to apply compressive stress to a section of the cross-section to reverse tensile stress and prevent flexural cracking.

In this thesis, prestressing is applied with a high-strength steel cable passing through the lower flange of the steel beam in a position eccentric to the strong geometric axis. The material requirements for prestressed steel beams were lower than conventional steel beams. The proposed cold-formed prestressed beams can be used for new applications in industry, especially when increased load-bearing capacity and reduced deformations are desired.

Figure 1.1 : Cold-formed steel members in construction (CSSBI, 2021).

1.2 Aims

This thesis was based on the following objectives in order to better understand the behavior of cold-formed steel beams:

1. Simulate the behavior of the proposed beam during the various loading phases using analytical and numerical modeling.
2. Detailed analysis and commentary of the extracted numerical results.
3. Determination of the parameters of the prestressed cable contribute to the carrying capacity of the system and further improvement of them.
4. Provide recommendations for further research.

1.3 Methodology

The following steps make up the research techniques utilized to accomplish the aforementioned goals:

Literature Review: A survey of the literature on cold-formed steel members and prestressing methods is conducted.

Analytical modeling: Both the cross-sectional and member levels of prestressed cold-formed steel beam mechanical behavior are investigated. In this manner, the behavior of the under-researched beams in terms of linear elastic behavior is established during the prestressing and applied vertical loading phases.

Numerical modeling: The main stages of numerical modelling are (i) elastic buckling analysis, (ii) generation of input files, (iii) FE simulation, (iv) data extraction, (v) data analysis, and (vi) post-processing.
The ABAQUS application was used to analyze the system using finite element (FE). After that, a parametric FE analysis is conducted to look at the important control parameters. Various combinations of beam geometries, cable sizes, and prestressing levels are modeled for this purpose in order to determine the ideal combination of attributes.

1.4 Outline of the thesis

This thesis is structured according to the methodology presented in section 1.3 and follows the objectives of section 1.2.

In chapter 2, the literature review is presented. All the necessary knowledge for understanding the mechanical behavior of the system is provided, which is derived from previous research on the two driving principles of the proposed structural system, namely prestressing and cold forming of steel.

In Chapter 3, the basic characteristics of the proposed system (structural elements, section geometry, hole geometry, member restraints) are presented, the axial stress levels at the critical points of the section and the moment-strain relationships at both loading stages are defined. In addition, the prestressing force and bending moment of the critical cross-section are determined.

In Chapter 4, the system is modeled using FE modeling. The basic characteristics of the finite element model (material response, boundary conditions, connection mode) are described.

In Chapter 5, the mechanical behavior of the proposed system at various loading stages is analyzed and the origin of the structural advantages obtained is identified. In particular, the contribution of the key parameters of the system is investigated, with the ultimate goal of maximizing them. A set of parametric studies is provided that investigate the influence of characteristics such as cable size and number of openings.

In Chapter 6, summarizes the findings of this study and conclusions are drawn. The contribution of this work to the field of structural engineering is then described and recommendations for future research are provided.

Chapter 2 - Literature Review

2.1 Introduction

In the present chapter, all data and findings of previous research on cold-formed prestressed steel beams were collected. More specifically, the first part of the literature review presents the prestressing technique, its benefits on the load-carrying capacity, performance and functionality of the system. The second part focused on the characteristics and properties of cold prestressed steel members and the instability phenomena that affect these members. Finally, the third part deals with the techniques of elastic buckling analysis and the summary conclusions of the chapter are presented.

2.2 Prestressing Technologies

Prestressing techniques are widely used in concrete structures. Nowadays, significant efforts are being made for applications in steel as well. In this section, the advantages of using these technologies in steel members are presented. In general, the objective of prestressing is to strengthen the member by introducing stresses at weak points in order to completely or partially neutralize the stresses expected to be generated by the applied load.

2.2.1 Historical development

The concept of prestressing has been applied throughout history and to most building materials such as wood, masonry, metals and concrete. It has been used for both common small-scale objects and large-scale structures. Today, it has become inextricably linked to the construction of large spans, such as prestressed bridges, due to the advantages achieved in structural performance, functionality and load-carrying capacity.

The principle of prestressing is estimated to date back to about 3500 years ago, as Casson (1971) and Torr (1964) illustrate Egyptian vessels built at that time in which the hull, piers and ropes formed structures to avoid 'hogging', i.e. negative curvature in the hulls. These hull structures were prestressed with twisting ropes, as shown in Figure 2.1.

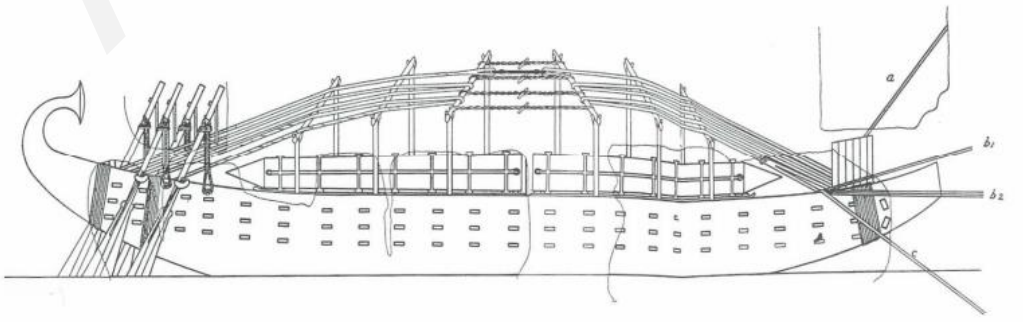

Figure 2.1: Egyptian barge prestressed by twisting ropes (Casson, L, 1971).

The construction of the large wheel by George Ferris in the late 19th century is also noteworthy. The wheel was 76m in diameter and was built for the 1893 World's Columbian Exposition in Chicago (Fincher 1983) to surpass the Eiffel Tower built for the 1889 Paris Exposition. The wheel had thirty-six cars, each of which was designed to carry sixty people on a leisurely two-turn, twenty-minute ride. The large wheel was prestressed by the tension of the cable rays as shown in Figure 2.2.

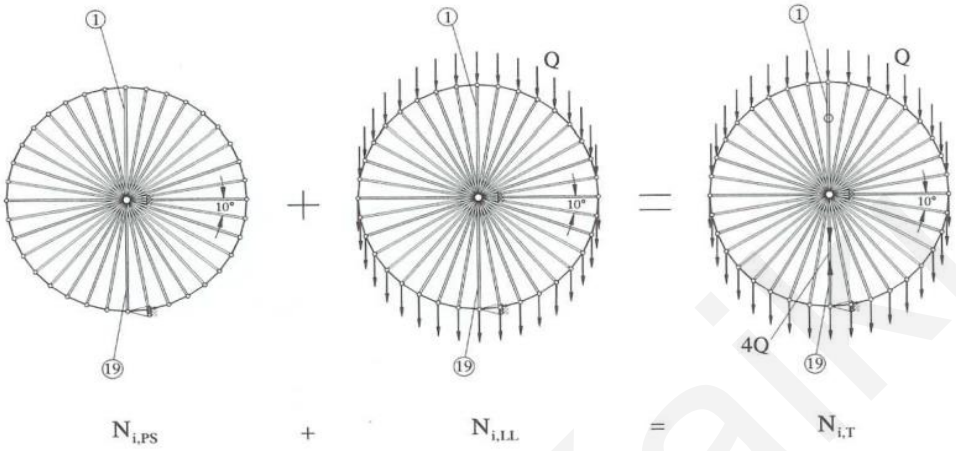

Figure 2.2 : Ferris wheel analysis by Johnson et al., 1894.

The same technique used by the Egyptians is used today to prestressing the blade on a traditional saw.

2.2.2 Prestressed steel structures

The prestressing technique was known only for reinforced concrete, but Dischinger, (1949) and Magnel, (1950) recognized the importance of using prestressing in steel beams and it was used both for the construction of new structures and for the strengthening of existing ones. (Troitsky, 1990) made a significant contribution by making suggestions on how to analyze and design prestressed bridge, slab, and beam systems. He estimated that prestressing steel can lead to material savings of 10-30%.

Prestressed steel has primarily been used for bridge construction, and roof structures have only rarely used it.. Many prestressed steel structures have been built around the world, particularly in the USA, Russia and Germany, which shows that the structural and economic advantages are many compared to non-prestressed systems. Indicative improvements in load-bearing capacity and reductions in deformations have been noted in structures incorporating prestressed residual columns (Saito and Wadee, 2008, 2009, 2010; Osofero et al., 2012; Yu and Wadee, 2017; Wadee et al., 2013) and prestressed steel arches (Clarke and Hancock, 1991).

Other modern example of prestressed structure are reconfiguration of the Sydney Olympic Stadium roof structure and the Five Star Aviation Hangar at Brisbane Airport. One of the oldest and most famous prestressed steel structures is the Britannia Bridge (Figure 2.3) over the Menai Straits. Constructed by Robert Stephenson in 1850, it was 1380ft long, with two main spans of 460ft and two side spans of 230ft, utilizes rectangular tube girders to carry

the railway tracks within the girders 7. The Britannia Bridge used a form of prestressing method called the "pre-deflection" method, which forces a deflection in the direction that will produce a moment countering the applied loading.

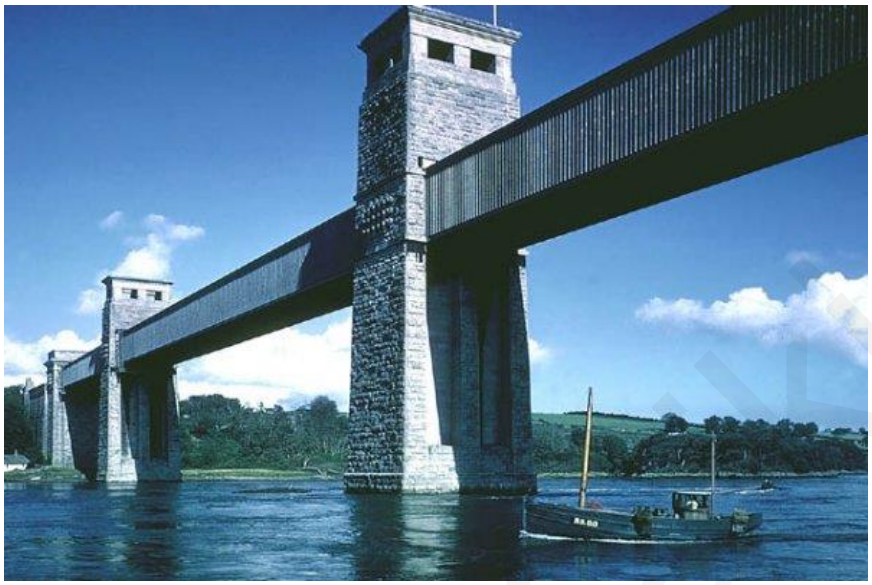

Figure 2.3: Britannia Bridge over Menai Straits. Photo taken from Encyclopedia Britannica.

2.2.3 Steel VS Concrete

As already mentioned in sections 2.2.2 and 2.2.3 above there are numerous advantages to using prestressing in steel over using it in concrete. However, the most widespread application of prestressing remains that of concrete, while at the same time significant steps are being taken to apply it to steel.

Steel, as a material, has a higher cost by weight than concrete, but the construction is usually shorter and requires less labor. In contrast, concrete requires more labor, cost and construction time. The strength of concrete is achieved after a period of 28days having near zero tensile strength. Unlike steel, which is admittedly stronger and has compressive and tensile strength in equal measure.
It is understood that there are also disadvantages in using steel instead of concrete. Steel sections are standardized and deviating from the standard requires additional construction costs. Also, the prestressing support conditions in steel sections require additional materials such as anchors and reinforcements, increasing the cost. Finally, concrete is easily formable, while it is extremely difficult and costly to achieve the same result for steel.

2.2.4 Prestressed bare steel beams

Prestressed bare steel beams are the most representative application of prestressing in cold-formed steel beams. The prestressing methods for steel beams were recommended by Subcommittee 3 of the ASCE-AASHO Joint Committee on Steel Flexural Members (1968) and are as follows:

1. Prestressing by means of high strength cables or rods anchored to the ends of the beam in question.
2. Prestressing by stressing hybrid beam elements - very similar to the prestressing technique. However, instead of concrete, high-strength steel plates are used.
3. "Preflex" prestressing where the beam is prestressed (Preflex) and uses the two main construction materials in their most ideal state - steel in tension and concrete in compression.

The purpose of prestressing is to introduce initial stresses within the steel element that compensate for the stresses resulting from the imposition of an external load. As shown in Figure 2.4 (a-b), the overall distribution of axial stresses includes three main components, axial compression and buckling caused by the initial prestressing force Pi and the buckling component caused by the applied bending moment M.

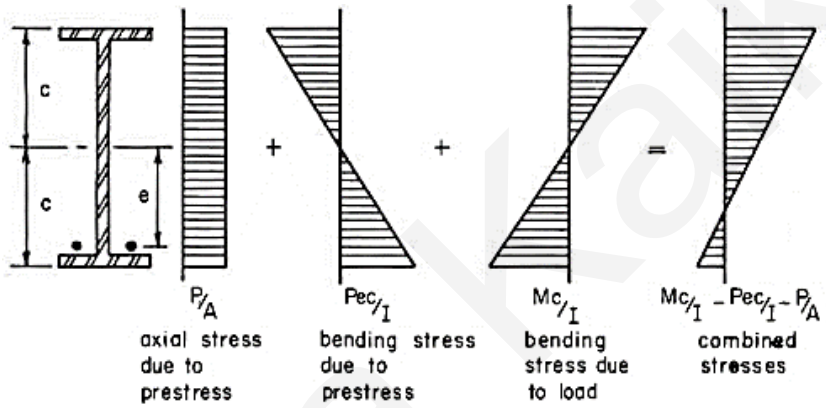

(a) Doubly-symmetric profile

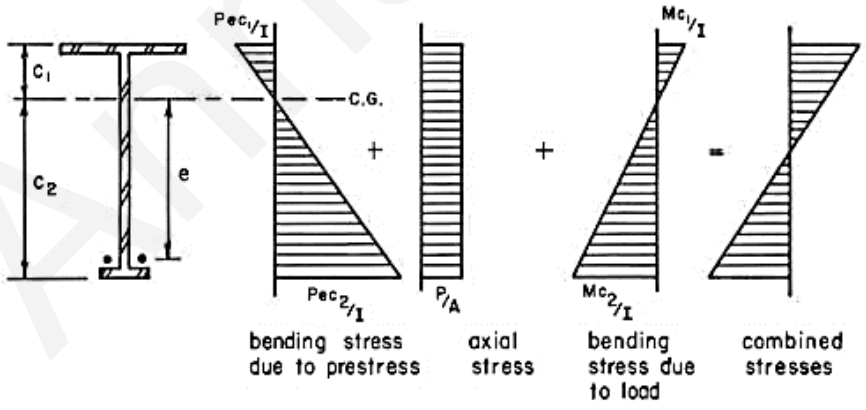

(b) Mono-symmetric profile

Figure 2.4: Axial stress distributions in prestressed (a) doubly-symmetric and (b) mono-symmetric steel girders. Adopted from Hoadley (1967).

The total axial stress levels at the top σt and bottom σb of the end fibers are calculated by superimposing the components, i.e:

$$\sigma_t = -\frac{P_i}{A_s} + \frac{\mathrm{P_i e}}{\mathrm{S_t}} - \frac{M}{\mathrm{S_t}}, \tag{2.1}$$

$$\sigma_b = -\frac{P_i}{A_s} - \frac{\mathrm{P_i e}}{\mathrm{S_t}} + \frac{M}{\mathrm{S_t}}, \tag{2.2}$$

where As is the cross-sectional area of the steel; $St=I_s/y_t$ and $Sb=I_s/y_b$ are the elastic section moments corresponding to the first yielding of the top and bottom end fibers respectively, with I_s the second moment of the cross-sectional area of the steel around the strong bending axis.

The geometry of the cross-section plays a crucial role in the effectiveness of the prestressing force Hoadley (1968) and Troitsky et al., (1989). More specifically, if the cross-section profile is symmetrical, the distribution of individual stresses is symmetrical due to the centroid axis located at the center of the cross-section but the overall stress distribution is non-symmetrical as shown in Figure 2.4 (a). When the cross-section profile is monosymmetric, the distribution of individual stresses is not symmetrical due to the centroid axis located in the upper half of the cross-section but the overall stress distribution is symmetrical as shown in Figure 2.4 (b). Here it is worth noting that due to the centroid axis located higher up, the eccentricity of the cable is higher and thus the prestressing is more effective.

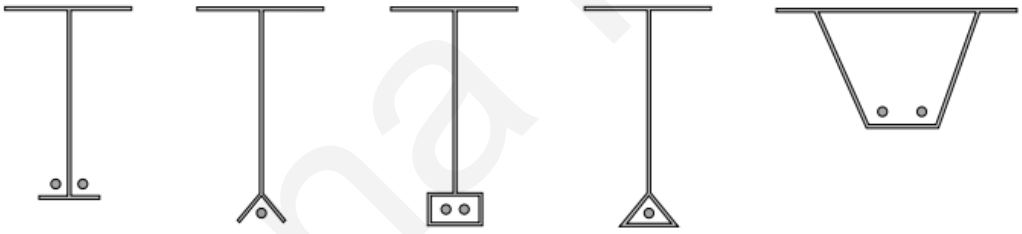

Figure 2.5: Cross-section profiles of mono-symmetric prestressed steel beams.

In addition, the profile of the cable also plays a decisive role. Hoadley (1968) concluded that a straight cable profile, where the cable is below the centroidal axis, results in a constant eccentric prestressing force and a uniform torsional moment along the beam, as shown in Figure 2.6 (a). In contrast, a parabolic cable profile, as shown in Figure 2.6 (b), results in a variable eccentric prestressing force, better reflecting the behavior of the beam under applied external loading.

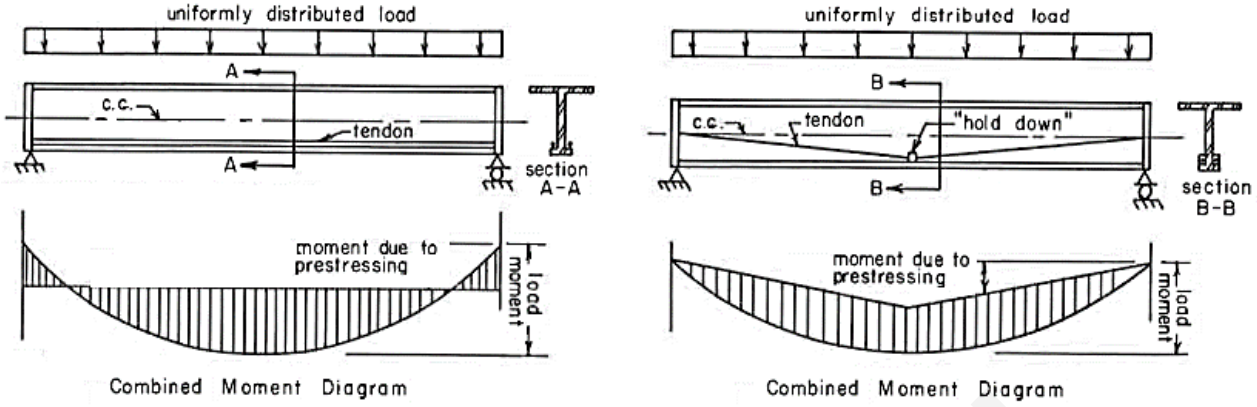

(a) Straight cable profile *(b) Parabolic cable profile*

Figure 2.6: Configuration and bending moment diagram corresponding to (a) straight and (b) parabolic cable profiles in prestressed steel beams. Adopted from (Hoadley, 1967).

2.3 Cold-formed steel members

In this section, the advantages of cold-formed steel members are presented. Cold-formed steel sections are increasingly used, offering more efficient and cost-effective solutions in construction. Moreover, their design is nowadays facilitated by modern analysis techniques and design methods.

2.3.1 Cold-formed steel in construction

The use of cold-formed steel members is not a new manufacturing method but has been used in North America for over 100 years. The use of cold-formed steel in the construction industry began in the 1850s in the United States and England. The use was initially experimental and limited to a few basic structures. Today, in both the United States and England, it is used for the construction of residential and non-residential structures (educational, commercial and industrial facilities).

2.3.1.1 Production techniques

The steps to be followed for the production of cold formed steel are: The steelmakers first melt the raw steel in a large furnace. After the raw steel has been converted to liquid form, it is allowed to cool slightly. It is then physically pressed by rollers at a low temperature to make it thinner and stronger. The low temperature makes the steel stronger and more durable compared to hot formed steel formed at high temperature. After the steel has cooled down, it is removed from the forming machine.

The thickness of cold formed galvanized steel, usually ranges between 0.9 mm to 3.2 mm for wall beams and floor joists and 1.4 mm to 3.2 mm in the case of purlins and cladding rails (Davison et al., 2012). The height of cold formed steel sections usually ranges from 50 mm to 300 mm (Trebilcock, 1994).

The disadvantage of cold-formed steel compared to hot-formed steel is the difficulty of production. The steel is not particularly malleable, especially at cold temperatures or at room temperatures. Of course, the forming process offers great flexibility in terms of the final shape of the cross-section and heat is not necessary to shape the cross-section.

Today, a wide variety of steel sections and thicknesses are available to meet the needs of modern structural applications. Today, there is a wide variety of both geometrically simple and more geometrically complex cross-sections to meet the needs of modern structural applications. The Swage and Zeta beam in Figures 2.8 (c) and (g) belong to the category of more geometrically complex cross-sections. The complexity of the cross-sectional shape leads to an increase in local instability resistance and lload-carryingcapacity.

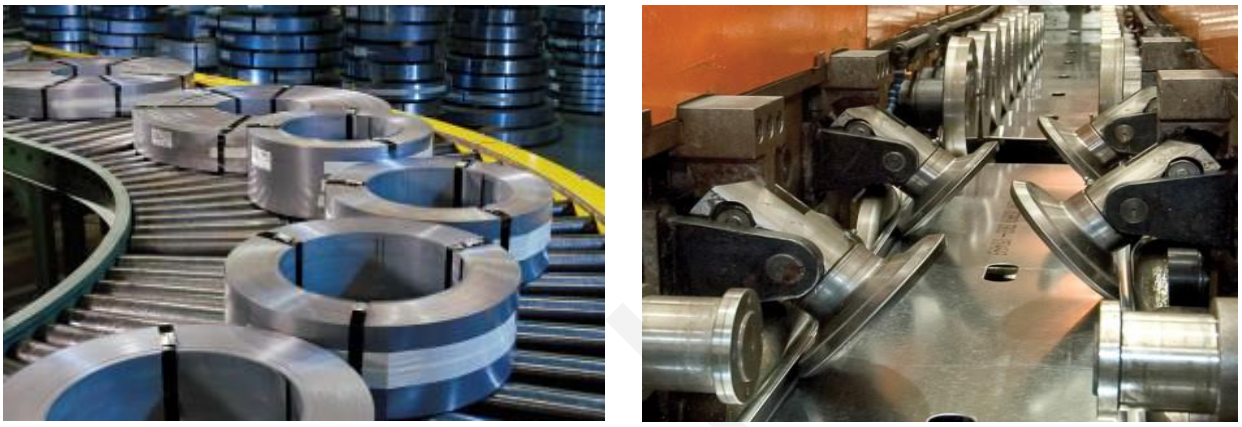

Figure 2.7: Production of cold-formed steel members using roll forming.

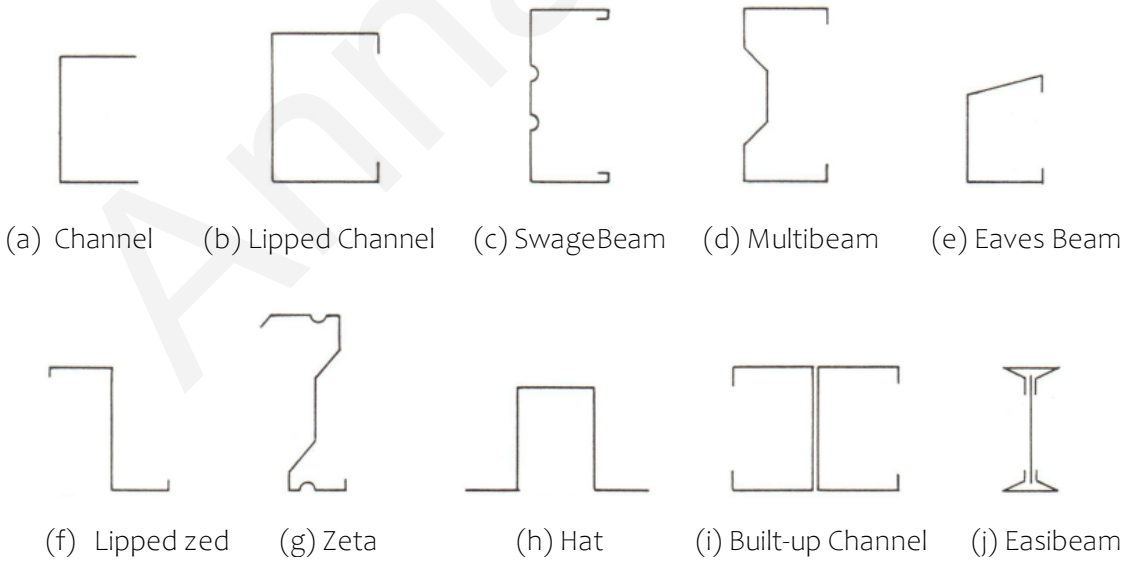

Figure 2.8: Examples of cold-formed steel cross-section profiles.

2.3.1.2 Effect of openings

The application of cold-formed steel (CFS) has been successful in the construction sector due to the significant load-bearing capacity achieved despite the limited thickness. However, CFS structural elements are still subject to continuous modifications and improvements in order to achieve better flexural strength since there is increased susceptibility due to thin walls. In addition, steel, as a material, has a higher cost by weight than concrete, but the construction is usually shorter and requires less labor so it is economically advantageous. The creation of openings also contributes to the reduction of the final cost but it must be taken into account that the final strength of the section is also affected.

The effect of openings on the cross-section depends on several factors, such as hole spacing, size, location, and arrangement. In general, openings may modify the local and deformation half-wavelengths of elastic buckling and possibly the critical elastic buckling loads. Experimentally, slotted openings appear to have little effect on ultimate strength, although ductility is reduced in some cases (Moen, Schafer, 2008). The American Iron and Steel Institute (AISI) design equations have been developed over the past four decades for columns with openings.

The presence of staggered slit-like perforations in cold-formed steel (CFS) beams is a new approach and is used in light steel construction with the aim of improving both fire and energy performance. However, cracks in the log reduce the bearing capacity of the beams with the weakened part of the log affecting the ultimate bending, shear, compression and their combined action. It also leads to a reduction in shear capacity of up to 70% compared to solid CFS beams (Degtyarev, Degtyareva, 2016). Finally, it was found that the influence of staggered slot-shaped perforations on the local buckling strength is relatively small, with a maximum reduction value of 11%.

In general, the presence of openings can modify the buckling shape of a member, can either increase or decrease its critical elastic buckling stress as well as increase the length of a stiffened member relative to the length of the hole. When the hole is wide compared to the width of the plate ($h_{hole}/h=0.66$) and L/L_{hole} is small, the elastic bending stress of the plate with the hole is up to 7% higher than that of the plate without the hole.

Therefore, it is concluded that the elastic flexural behavior of a rigid element with a single hole depends directly on the size of the hole. As for the case of multiple openings, the elastic flexural behavior depends on the distance between the openings. Its increase or decrease is determined by the ratio of the width of the hole to the width of the plate. (Moen, 2008).

2.3.1.3 Advantages of cold-formed steel

The main advantages of using cold-formed steel members can be categorized as follows:

1. Rapid construction process due to the use of prefabricated elements
2. High strength-to-weight ratio and coverage of large openings
3. Low weight which also facilitates handling of members
4. Good quality works
5. Long-term corrosion resistance by galvanizing cold formed steel products
6. Dimensional stability - does not expand or shrink in humid conditions

7. Recycled content at 25%
8. Reduced waste of materials during manufacture
9. No form work needs

2.3.1.4 Applications in building construction

The application of cold-formed steel members has expanded significantly in construction. As primary members, they are used in light steel framing in cases of residential and low-rise apartment buildings. As secondary members they can be used in industrial, commercial and agricultural facilities providing lateral restraint to the primary members. Some of the main applications are:

1. Load-bearing walls for the transfer of lateral loads
2. Non-load-bearing walls for shaping the building envelope
3. Roof and wall systems (industrial, commercial and agricultural buildings)
4. Steel shelves for supporting storage pallets
5. Structural members for flat and space beams
6. Frameless structures with stressed skin: Use corrugated sheets or sheet metal profiles with rigid ends for small structures with net span up to 30 feet without internal framing.
7. Floor decking, roof decking and wall systems
8. Hybrid systems: Combination with other materials such as precast concrete, wood frame and structural steel.

2.3.2 Material behavior

The material properties are the cornerstone for the final performance of steel elements. What determines the material properties and thus the final performance of the elements is the forming process. Cold-forming imparts properties to the steel member that differ significantly from those of hot forming and are to be explained in detail in this section.

2.3.2.1 Stress–strain response

The response of hot-formed steel compared to the response of cold-formed steel shows significant differences. First, the stress-strain response of cold formed steel shows a more rounded shape, with no clear yield point and a significant hardening period (Figure 2.9). In contrast, the hot formed steel response clearly shows the yield point and yield plateau (Figure 2.10). Since the yield point in cold-formed steel is not determined, it can be obtained by the offset method, with an offset of 0.2%, as shown in Figure 2.9. The rounded response is attributed to the cold working process, which, has two additional effects on the material behavior that will be analyzed below.

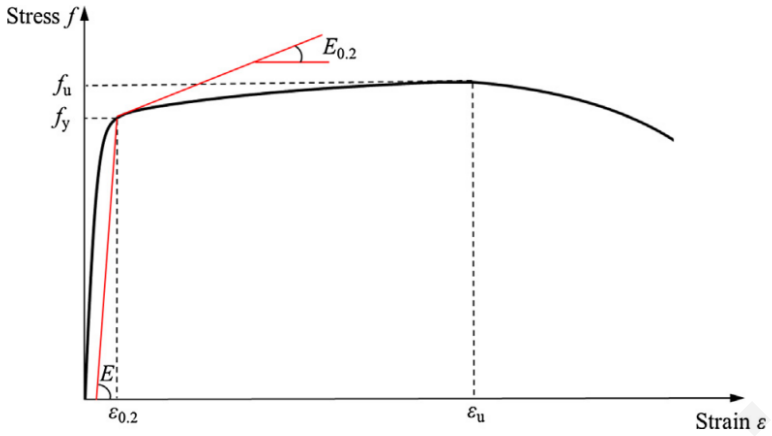

Figure 2.9 : Stress–strain curve for cold-formed steel. (Gardner and Yun, 2018).

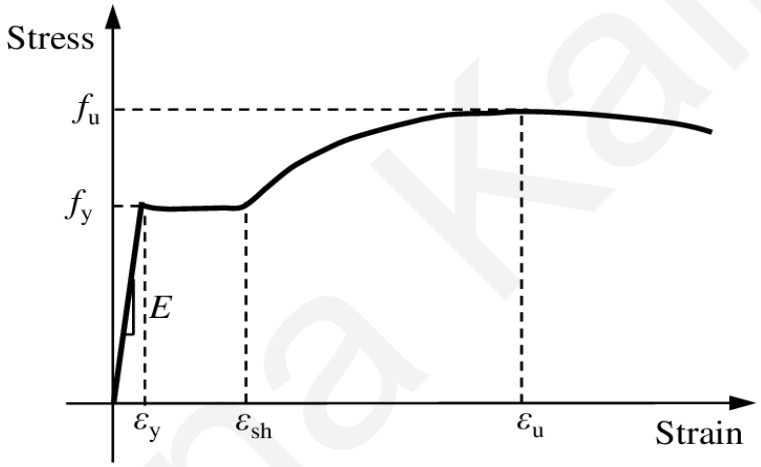

Figure 2.10 : Stress–strain curve for hot-formed. (Yun and Gardner, 2017).

2.3.3 Buckling effects

Buckling is the phenomenon of large deformations of the structural element in the plane of application of the load that causes them - for small changes in the load, resulting in the loss of elastic stability of the member. This phenomenon occurs mainly in members under compression. More specifically, cold-formed steel members are potentially vulnerable to three main modes of elastic buckling local, distortional and global buckling, all of which belong to the local instability phenomena. Global buckling includes bending, torsion or bending-torsion buckling for columns and lateral-torsion buckling for beams.

The study of the buckling phenomenon is a complex analysis issue due to the fact that the phenomenon is directly influenced by the support conditions of the buckled member, the geometric imperfections and the eccentricity of the compressive load. Also, the geometry of thin walls makes steel members particularly vulnerable to the above-mentioned local instability phenomena.

Despite the complexity of buckling, advanced analysis techniques have been developed that allow the prediction of the above-mentioned phenomena and facilitate for the determination of the limiting strength of cold formed steel members by modern methods such as direct strength method (DSM).

The deformed shapes in cross-sectional and member planes corresponding to the fundamental bending modes of a thin-walled column with channel lips are illustrated in Figure 2.11, where the critical half-wavelengths Lcr are also indicated.

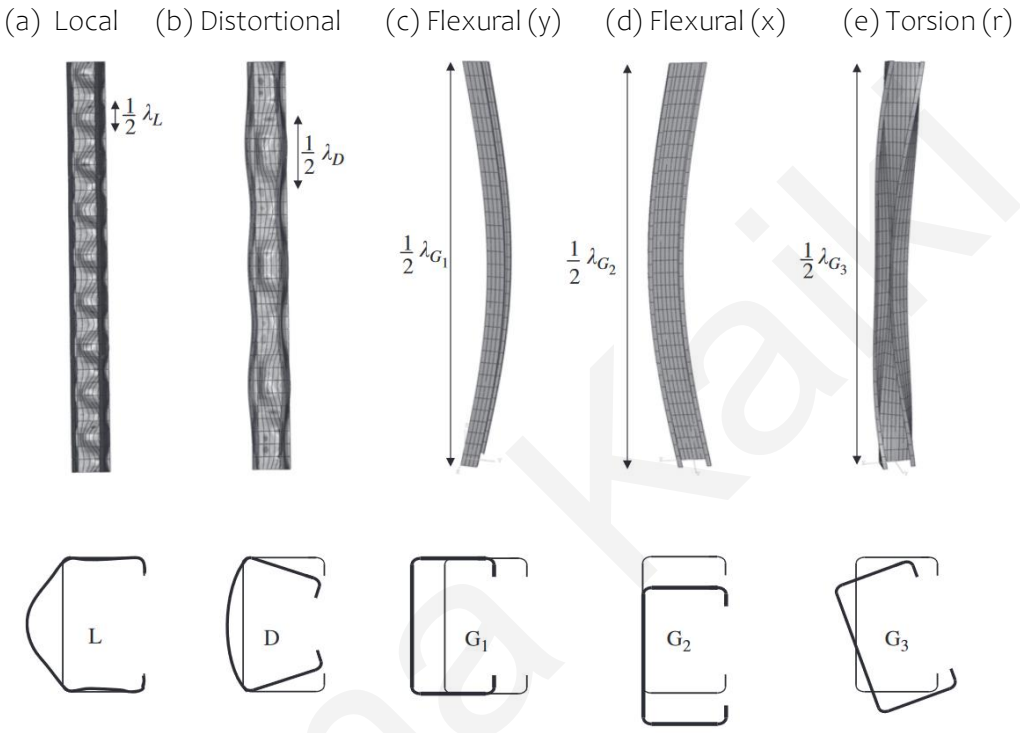

Figure 2.11: Fundamental buckling modes of a thin-walled lipped channel member subjected to axial compression; Lcrl, Lcrd, Lcre,y, Lcre,x and Lcre,r are the critical half-wavelengths for local, distortional, global flexural about the y–y axis, global flexural about the x–x axis and global Distortional buckling respectively. Adopted from Zeinoddini and Schafer, 2012.

2.3.3.1 Local buckling

Local buckling is the phenomenon in which the thin-walled member is subjected to lateral displacement of the cross-section walls (relative to the direction of compressive stress). In the European standards of Eurocode 3 (EC3), cross-sections subject to local buckling are classified as category 4. As a consequence of local buckling, the load-bearing capacity of the critical cross-section is reduced, leading to a reduction in the strength of the whole structural element. It should always be taken into account when designing cold-formed steel elements.

Figure 2.11 (a), shows the deformation of the cross-section, which is only with rotation and not displacement at the internal bending lines (e.g., corners) of the member (*AISI S100-16*, 2016). The critical half-wave length for local buckling is usually less than or equal in length to

the longest dimension of the cross-section subjected to compression. Variations involving increasing wall thickness, adding edges or reinforcement can significantly reduce the effect.

Test results show that the *AISI S100-16*, (2016) and *NAS (North American Specification)*(2001) the new NAS (2001) design methods provide reasonably satisfactory strength predictions for cold formed steel members. Also, the Direct Strength method provides the best test-to-predicted ratio for both slender and unslender specimens (Yu and Schafer, 2002).

2.3.3.2 Distortional buckling

Distortional buckling is a relatively new and less researched type of buckling compared to the others. It mainly affects members with stiffening edges (channel lips, Z-sections, hat, rack, etc.). As shown in Figure 2.11 (b), distortional buckling involves significant cross-sectional deformation, with a combination of rotation and displacement (AISI S100-16, 2016). The critical half-wavelength is greater than half-wavelength for local buckling and less than that for global buckling.

In addition, compared to local buckling, distortional buckling has significantly lower stiffness after buckling (Schafer and Peköz, 1999). If it is expected that the members will achieve a lower stress for local buckling than the stress for distortional buckling, distortional buckling may be ignored in the analyses. Members with wide flanges are deformed deformably, while those with narrow flanges are locally buckled. Members with narrow flanges, however, can fail in distortional buckling when reinforcements are added to the web (Ranawaka, T., 2006).

2.3.3.3 Global buckling

Global buckling includes flexural, torsional or flexural-torsional buckling for columns and lateral-tortional buckling for beams. In Figures 2.11 (c)-(d), the cross-section is laterally deformed but the shape remains unchanged. In Figure 2.11 (e), which is for lateral-torsional buckling, the cross-section is deformed out of plane and rotated about its shear center (*AISI S100-16*, 2016). The critical half-wave length for the cases of global buckling is equal to the unsupported length of the beam.

The limitation of the phenomenon can be achieved by limiting the lateral deformations of the cross-section flange, mainly preventing lateral-rotational buckling. Similar to how floor plates are fixed under compression in cold-formed steel beams (Davison and Owens, 2012).

2.3.4 Initial geometric imperfections

Initial geometric defects are the deviation of the member from the original "perfect" geometry and include local deviations (e.g. dents), bending, distortion and twisting of the cross-section (Schafer and Peköz, 1998a). It is an unavoidable characteristic of steel members and originates from factors such as fabrication, welding and transportation, affecting the stability, flexural strength, stiffness and load-bearing capacity of the member. Depending on the length of the member, two types of defects arise: (1) local defects in short members, (2) total defects in long members.

Since the defects affect the bending resistance and the ultimate bearing capacity, it is easy to see that they favor the early development of instability phenomena and must be carefully taken into account in the design. It is worth noting that the distribution of the initial geometric defects in the cross-section is non-uniform and the parameters affecting this distribution are forming, fabrication, material strength and geometric properties. It is widely accepted that the initial geometric defects play an important role in the nonlinear behavior of CFS members.

Schafer B.W., Peköz T., 1998a proposed empirical rules on the magnitude of imperfections having made an extensive survey from a wide range of measurements. The defects were categorized into two groups: (1) defects corresponding to local buckling of a stiff element and (2) defects corresponding to the maximum deviation from the straightness of a lip/absorbed flange (i.e. deformable buckling). The proposed rules apply to thicknesses less than 3 mm and to plate elements with a width-to-thickness (w/t) less than 200 and 100 for flaw types 1 and 2, respectively. Significant research work on the subject of defects was carried out by, Al Ali (2013 , 2014) who modeled the initial defects of thin-walled cold-formed pressed steel members with closed sections in MATLAB and performed nonlinear buckling analysis to determine the limit loads, Ungermann (2008) who dealt with the consistency of defect rules according to EC3 and Zeinoddini (2012) who introduced spectral representation approaches for simulating geometric defects in cold-formed steel members.

More specifically, Schafer and Peköz analyzed the frequency and amplitude of two types of local geometric defects shown in Figure 2.12, where d1 represents local buckling, while d2 represents distortional buckling. Based on the probabilistic analysis of the measured defects and using the Fourier transform, they evaluated the frequency of occurrence of the so-called "defect signal". Each mode of instability is characterized by half the wavelength. If the critical instability mode is determined using an elastic eigenmode analysis, then, for the critical defect, the frequency of occurrence is estimated and the corresponding maximum amplitude of that defect is also estimated. As a practical alternative, Schafer and Peköz proposed coded values for the maximum amplitude of geometric defects:

Local Buckling Mode: $d_1 = 6te^{-2t}$ or $d_1 \approx 0.006w$ (2.3)

Distortional Buckling Mode: $d_2 \approx t$ (2.4)

where w and t are the width and thickness of the relative wall. These "coded" values are more conservative than those obtained when the probabilistic approach is used.

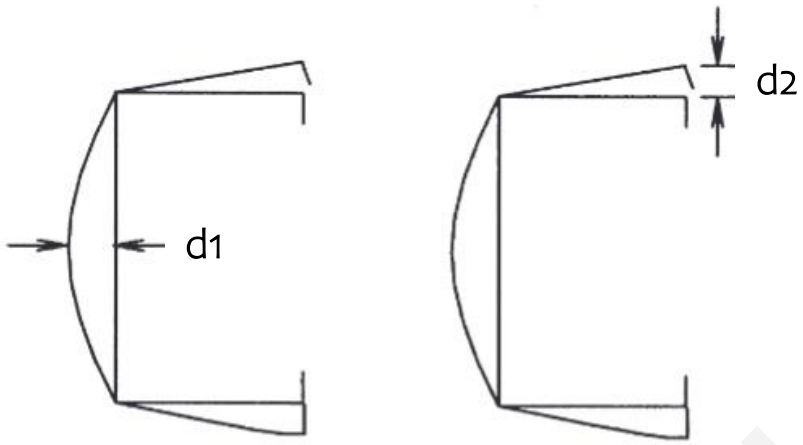

Figure 2.12: Definition of initial geometric imperfections for (a) local and (b) distortional buckling. Adopted from Schafer and Peköz, (1998a).

2.3.5 Elastic buckling analysis

Elastic buckling analysis methods can be used to determine the elastic critical buckling loads/moments i.e. the starting points of instability. In current design codes, such as North American (*AISI S100-16*, 2016). Australian/New Zealand (*Standards Australia*, 2018) and European (*EN-1993-1-3*, 2006), elastic critical buckling load/moments are used as reference loads for calculating the ductility and limit strength of cold-formed steel members.

The most popular methods for the design of cold-formed steel members are the direct strength method (DSM), finite element method (FEM), finite strip method (FSM), constrained finite strip method (cFSM) and generalized beam theory (GBT). In this thesis, the finite element method (FEM) and constrained finite strip method were used (cFSM).

2.3.5.1 Finite Element Method (FEM)

Finite Element Method (FEM) is such a numerical method that subdivides a complex space into a number of small, measurable and finite number of pieces, whose behavior can be described by simple equations. For finite element (FE) modelling in this case, plate or shell elements are used and the analysis is performed to determine the elastic buckling loads (eigenvalues) and buckling eigenmodes (eigenvectors).

The main advantage of the FE analysis is that all characteristics of the cold-formed steel member can be accurately modeled. Some of these characteristics are boundary conditions, moment gradients, openings, connections, and thickness variations along the member (Schafer, 2006). The main disadvantage of FE analysis is the visual inspection required to identify the characteristic buckling modes and classify them into local, distortional, and global buckling. This is a subjective and often time-consuming process.

Finite element simulation is carried out using software. In this thesis, the software ABAQUS was used.

2.3.5.2 CUFSM

CUFSM was developed by Ben Schafer in 1997 and is a combination of the Constrained and Unconstrained Finite Strip Method.

Cold-formed steel members are thin, lightweight and yet efficient. However, their thin walls make them particularly vulnerable to bending. Classical manual solutions for instabilities can be particularly difficult for more complex bending modes, especially when they ignore critical mechanical characteristics. The solution to this problem is achieved by using numerical methods such as the finite strip method (FSM).

The finite strip method (FSM) considers all possible instabilities in a cold-formed steel member when subjected to axial stresses, bending stresses or a combination of these. CUFSM is an open-source FSM program that performs analysis for a predefined number of half-wavelengths based on the assumption that the member is tensional along the member in half sine waves according to the following expression (Schafer, 2006):

$$\text{Buckling mode} = \text{2D mode shape} \times \sin\left(\frac{\pi x}{\text{half-wavelength}}\right) \qquad (2.5)$$

The constrained finite strip method, or cFSM, is an extension of the conventional FSM solution. The constrained finite strip method provides: (1) a modal decomposition stability solution, or (2) a conventional FSM stability solution for different modes of buckling (modal identification). Modal decomposition is achieved by forming a set of constraint equations describing a particular class of buckling (local, distortional or global). A stability study is then performed after constraining an FSM solution to a specific class of buckling.

Using the software requires simple steps from the user. First, the coordinates of the nodes, the connection of the members, the applied load and the support conditions of the tested cross-section are entered and finally CUFSM produces results about the stability of the cross-section. Thus, the user can fully understand the stability of cold-formed steel sections by having the combination of the traditional finite strip approach and the finite strip method with constraints.

2.4 Concluding remarks

The purpose of this chapter is to provide a complete description of the technical background of the prestressing techniques used to improve cold-formed steel elements.

The first part of the literature review presented a historical overview of prestressing techniques, their use initially in concrete and then in steel, highlighting the advantages of their use from the earliest stages of their application. The fundamental concept of prestressing is the introduction of stresses within structural elements that are of opposite sign to the stresses induced during the imposed external loading, in order to compensate for them. A comparison was then made between prestressed concrete and prestressed steel, with steel being superior to concrete in terms of efficiency and cost. In addition, the influence of key parameters on the prestressing efficiency, such as the geometry of the prestressed member cross-section and the cable profile, was investigated.

The second part of the literature review presented the basics of cold-formed steel, such as manufacturing techniques, its applications in structures, the advantages of its use, the behavior of the material, the influence of any openings and presented the buckling analysis. The manufacturing process of cold-formed steel members has a significant impact on the final behavior of the material. In particular, the low temperature makes the steel stronger and more durable compared to hot-formed steel. Next, the effect of instability phenomena on cold-formed steel members was examined. For this purpose, the characteristics of local, deformation and global buckling.

Finally, various types of elastic buckling analysis techniques were described for the determination of strength in cold-formed steel members. These techniques facilitate the understanding of the interactions between the different buckling modes and are essential for the development of more efficient and optimized geometries.

Chapter 3 – Concept and Analytical Modeling

3.1 Introduction

In this chapter, the innovative concept of improving the load-bearing capacity of cold-formed steel beams using prestressing techniques is discussed in detail. First, the main characteristics of the proposed prestressed beams and the assumptions made throughout this work are presented.

Then, the mechanical response of the system during the two loading stages, prestressing and vertical loading, is analyzed. The distribution of axial stresses in the critical cross-section during the two loading stages is studied and the advantages obtained are highlighted.

3.2 Concept

As already mentioned in section 2.3.3, cold-formed steel elements are superior to other materials due to their high strength-to-weight ratio, which makes them lighter and more economical as a structural solution. However, their thin walls make them particularly susceptible to instability phenomena, in particular local, distortional, and global buckling, which directly affects their load-bearing capacity.

In the proposed concept, prestressing techniques are used in order to delay the occurrence of the instability as mentioned above phenomena. The prestressing force is applied through a high-strength steel cable, which is in an eccentric position with respect to the strong geometric axis and passes through the bottom hollow flange of the steel beam, causing initial stresses in the member that are of opposite sign to those introduced during the applied loading.

The stresses imposed by the prestressed cable led to the development of compressive stresses at the bottom of the beam and tensile stresses at the top. The imposition of prestressing is for Stage I, while the imposition of vertical loading is for Stage II. In Stage II, the applied load is applied vertically at the top of the beam and results in the development of compressive stresses at the top of the beam and tensile stresses at the bottom.

The presence of the prestressed cable contributes to a significant reduction in the bending moment resulting from the distributed loading and a reduction in the vertical deformation of the system due to the bending effect. Therefore, the system thanks to the pre-stretched cable is able to carry loads of larger magnitude compared to the system without the pre-stretched cable. In addition, it is possible to use smaller cross-sections for a given capacity and span length requirement, resulting in material savings.

Finally, the proposed prestressed beams show improved operational performance. Potentially, they can be more widely used as dominant structural elements in the construction of buildings and other structures.

3.3 Principal Characteristics

3.3.1. Cross-sectional geometry

As already mentioned in previous sections, the cold-formed steel manufacturing process provides some advantages over hot-formed steel. It is faster, less expensive, and allows the manufacture of geometrically complex sections. These advantages are taken into account for the implementation of the proposed system; therefore, the steel beam is designed with two longitudinal stiffeners in the web at the top and bottom to resist local buckling of the cross-section and with openings in the bottom tread through which the prestressed cable will pass. The presence of the openings contributes significantly to the reduction in material and consequently in cost.

The geometry of the cross-section is essentially that of a lipped channel section and the proposed cross-section profile is shown in Figure 3.1, where the steel cable is located through the lower flange of the steel beam at an eccentricity e with respect to its strong geometric axis (x-x). Note that, the prestressing cable is eccentric with respect to the strong geometric axis but not with respect to the weak axis of the cross-section.

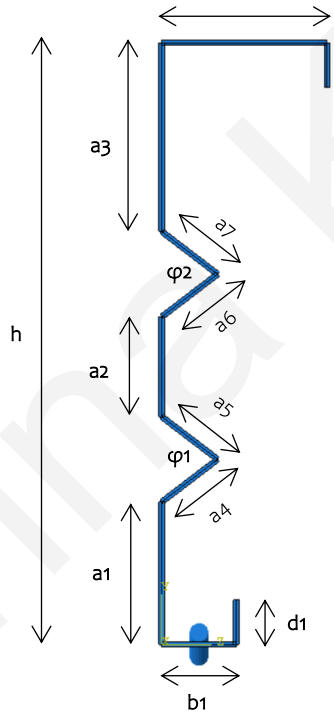

Figure 3.1: Reference cross-section profile of the prestressed cold-formed steel beam.

The geometric characteristics of the cross-section are shown in Table 3.1. where rc is the radius of the cable and t is the thickness of the steel beam.

h	325.0 mm	a2	40.0 mm
d1=d2	25.0 mm	a3	100.0 mm
b1=b2	90.0 mm	a4=a5	30.0 mm
t	30.0 mm	a6=a7	30.0 mm
a1	75.0 mm	Φ1=Φ2	70.0 °

Table 3.1: Dimensions of the reference cross-section profile; the symbols are defined in Figure 3.1

3.3.2 Structural system

The proposed prestressed system includes two structural members, namely the cold-formed steel beam and the high-strength steel cable, as shown in Figure 3.2. We assume that the studied members are assumed to be in a simply supported configuration.

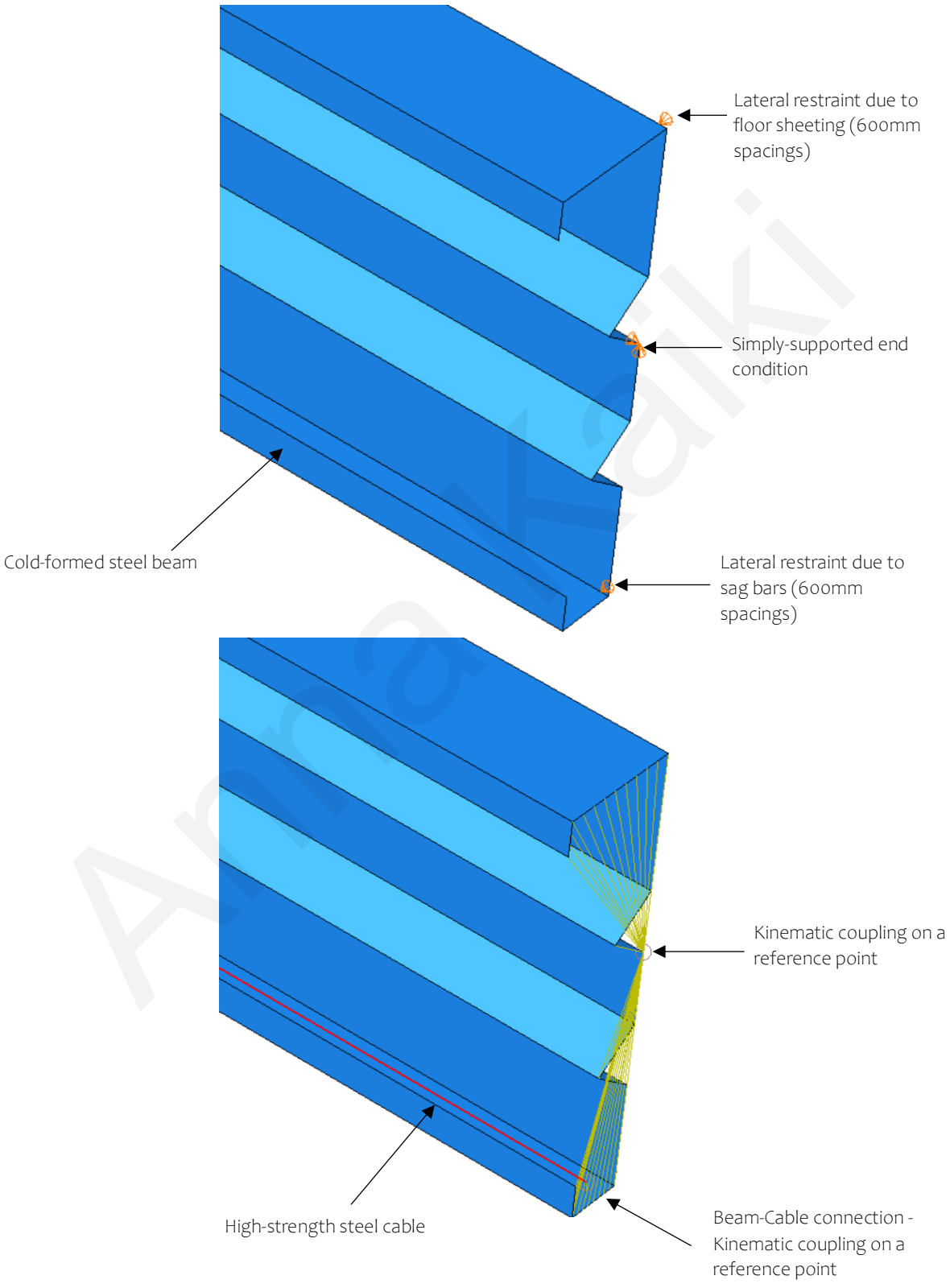

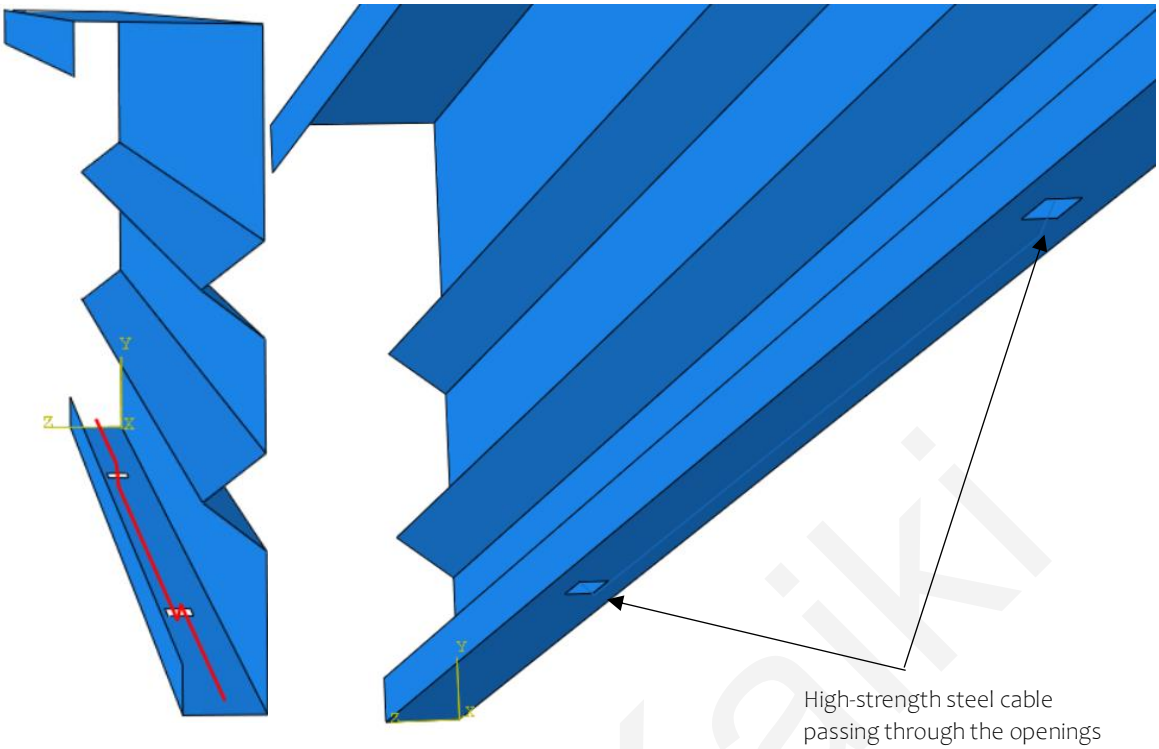

Figure 3.2: Primary features and restraints of the proposed prestressed structural system.

3.3.2.1 Cold-formed steel beam

In this thesis, the lower end of the beam flange is assumed to be inseparably connected to the tread but the connection medium is not considered. In addition, lateral supports are provided by the presence of floor sheeting and sag bars connecting the top and bottom flanges to those of the adjacent cold-formed beam. These lateral restraints, within the simulation, are implemented using boundary conditions at 600mm intervals along the length of the beam.

3.3.2.2 High-strength steel cable

The proposed system, in addition to the cold-formed beam, consists of the high-strength steel cable housed within the bottom flange of the cross-section. The cable is stretched using a lifting mechanism and anchored at both ends of the beam, transferring the prestressing force to the beam. The anchoring system, however, is not studied here.

Along the length of the beam, the cable passes through the bottom tread through rectangular openings. More specifically, starting concentrically, the cable is straight at the top of the tread, at the first hole it slopes to pass through it and continues at the bottom of the tread again in a straight line. At the next hole it is again inclined, goes through it and becomes straight again at the top of the tread. This is repeated along the entire length of the carrier. Finally, the cable can be freely elongated.

3.3.3 Member restraints

The presence of the cable enhances the stability of the proposed system by providing a number of restraints. In particular, the cable contributes significantly to enhancing the stability of the system by limiting the overall bending during the two loading stages. The axial compression results from the prestressing force, in both loading stages, whose line of action follows the deformation of the beam. This has been investigated in the work of Gosaye, J. et al. (2016) and Wang, J. et al. (2017) and it was shown that the presence of the cable reduces the effective length of the beam and increases the bending strength.

In addition, the lateral restraints imposed at 600mm intervals along the length of the beam limit buckling around the strong geometric axis (x-x) of the cross-section, thus preventing asymmetric buckling phenomena and lateral displacements of the bottom flange of the beam.

3.3.4 Losses of prestress

Short-term prestressing losses occur during the transfer of the prestressing force from the cable to the steel beam (e.g., due to anchor slip, friction and elastic shortening of cold-formed steel beams), while long-term losses occur during the life of the prestressed members (e.g., from loosening of the prestressed cable and creep of the steel). Prestressing losses, lead to reduced final system performance.

It is understood that losses must be taken into account when calculating the actual prestressing force. In the present work, prestressing losses are not taken into account. Therefore, the initial prestressing force is simply taken as the actual prestressing force.

The magnitudes of these losses depend in part on the specifications of the components of the prestressed system, which are usually provided by the manufacturer, as mentioned in section 2.2.7. Creep is generally very low in the case of steel and, due to the profile of the cable, the friction between the cable and the steel beam can be considered negligible.

3.4 Loading Stages and analytical modeling

In this chapter, the mechanical behavior of simply supported prestressed cold formed steel beams is studied during two stages, prestressing and applied loading. Stage I, involves the transfer of the prestressing force from the prestressed cable to the steel beam. Stage II, involves the application of the uniformly distributed load to the top of the steel beam. Analytical expressions are used to describe the elastic behavior of the beam, the stress levels at the critical cross-section, i.e., at mid-span, and the load-deformation response of the beam.

The final response of the system depends largely on the stress distribution, which, especially in the case of cold-formed steel beams subjected to a combination of axial load and bending moments, can be considered the key control parameter (Torabian, S. et al. 2014a, Torabian, S. and Schafer, B. W., 2018).

3.4.1 Stage I: Prestressing

Stage I concerns the prestressing force and its transfer from the cable to the steel beam. The cable shall be tensioned using a jack mechanism and anchored to both ends of the beam. Through the anchoring mechanism, the prestressing force is transferred from the cable to the cold-formed steel beam.

More specifically, the stress distribution, shown in Figure 3.3 (c), can be broken down into a uniform compression, (Figure 3.3 (a)) and a linearly varying stress distribution (Figure 3.3 (b)).

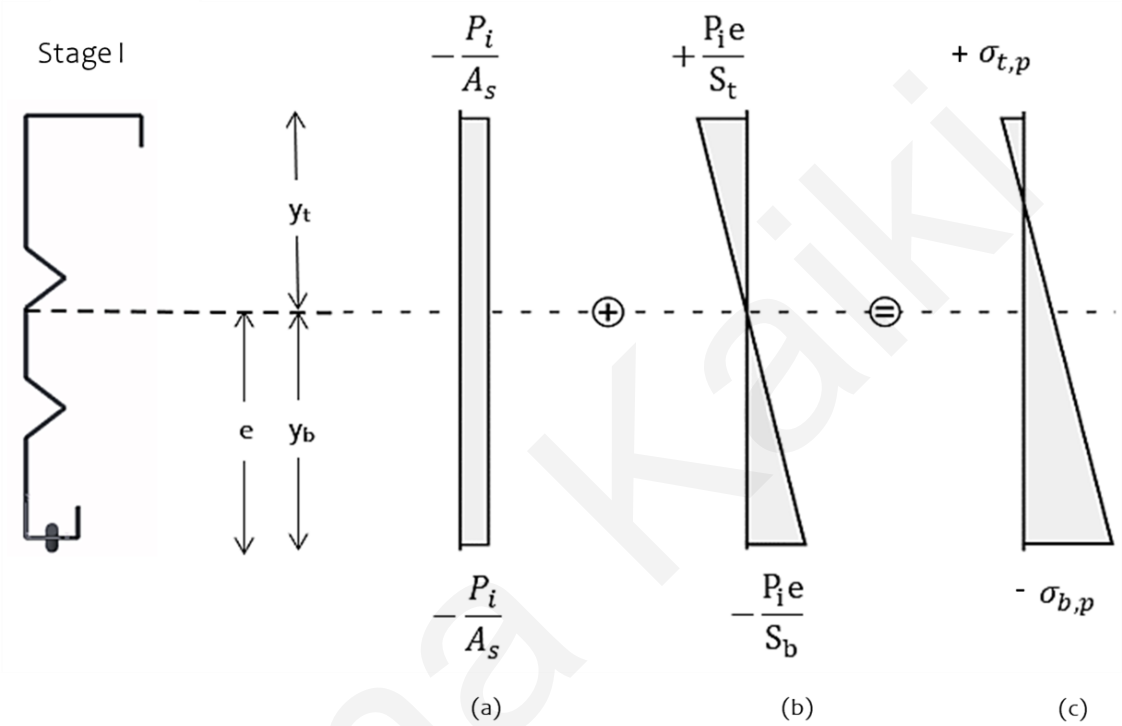

Figure 3.3 : Axial stress distribution at the critical cross-section at the end of Stage I. (a) Uniform compression component due to Pi , (b) bending component due to the eccentricity at which Pi is applied and (c) net axial stress distribution.

The latter is a result of the eccentricity e to which the initial prestressing force is applied. The superposition of the two components leads to a net tensile stress in the top flange $\sigma_{t,p}$ and a net compressive stress in the bottom flange $\sigma_{b,p}$, as illustrated in Figure 3.3 (c), therefore:

$$\sigma_{t,p} = -\frac{P_i}{A_s} + \frac{P_i e}{S_t}, \tag{3.1}$$

$$\sigma_{b,p} = -\frac{P_i}{A_s} - \frac{P_i e}{S_b}, \tag{3.2}$$

where A_s is the cross-sectional area of the cold formed steel beam, $S_t=I_s/y_t$ and $S_b=I_s/y_b$ are the elastic cross-sectional moduli corresponding to the first yielding of the top and bottom flanges respectively, with y_t and y_b being the distance of the centroid from the upper and lower end fibers respectively, and Is being the second moment of the cross-sectional area of the cold formed steel beam around its strong geometric axis.

The strength of the cross-section is limited by the compression plane at the bottom flange. The initial prestressing force is therefore limited by either yielding or local/distortional buckling (depending on the ductility of the cross-section) of the bottom cross-section of the cross-section. Therefore, the possible failure of the lower flange of the steel section during prestressing must be taken into account.

The uniform torsional moment Pie, causes pre-cambering, i.e. vertical upward deformation of the beam. The pre-camber contributes to the functional performance of the proposed system, as it eliminates part of the deformations induced in stage II of the applied load. At the end of the prestressing stage, the relationship between the initial prestressing force and the vertical deflection at mid-span δ:

$$\delta^{I}{}_{mid} = -\left(\frac{L^2}{8E_s I_s}\right) P_i e, \tag{3.3}$$

where L and Es are the length of the girder and the Young's modulus of elasticity of the cold-formed steel respectively.

3.4.2 Stage II: Imposed vertical loading

Stage II involves the application of an externally applied vertical load (dead load and payload carried by the member after application of the prestressing), in the form of a uniformly distributed load q, which causes a maximum bending moment (positive) $M_{max} = \frac{qL^2}{8}$ at the critical section, i.e. at the mid-span.

As the beam deforms vertically, the cable is stretched further and therefore an additional axial force is induced in the cable as it is below the neutral axis of the cross-section. This force is transferred back to the steel beam at the anchorages at the ends as an incremental prestressing force ΔP, which results in an additional uniform torsional moment equal to ΔPe, as shown in Figures 3.4 (b) and (c).

A reduction of the applied torque in the middle of the opening is achieved. Figure 3.4 shows the stress distribution at the mid-span of the Stage II beam and also includes the stress distribution from the end of Stage I (Figure 3.4 (a)). In more detail, a linearly varying stress distribution around the cross-section centroid as a result of M_{max} (Figure 3.4 (b)) and two stress distributions (compression and bending) due to ΔP (Figures 3.4 (c) and (d)) are shown, which has the same effect as Pi during Stage I.

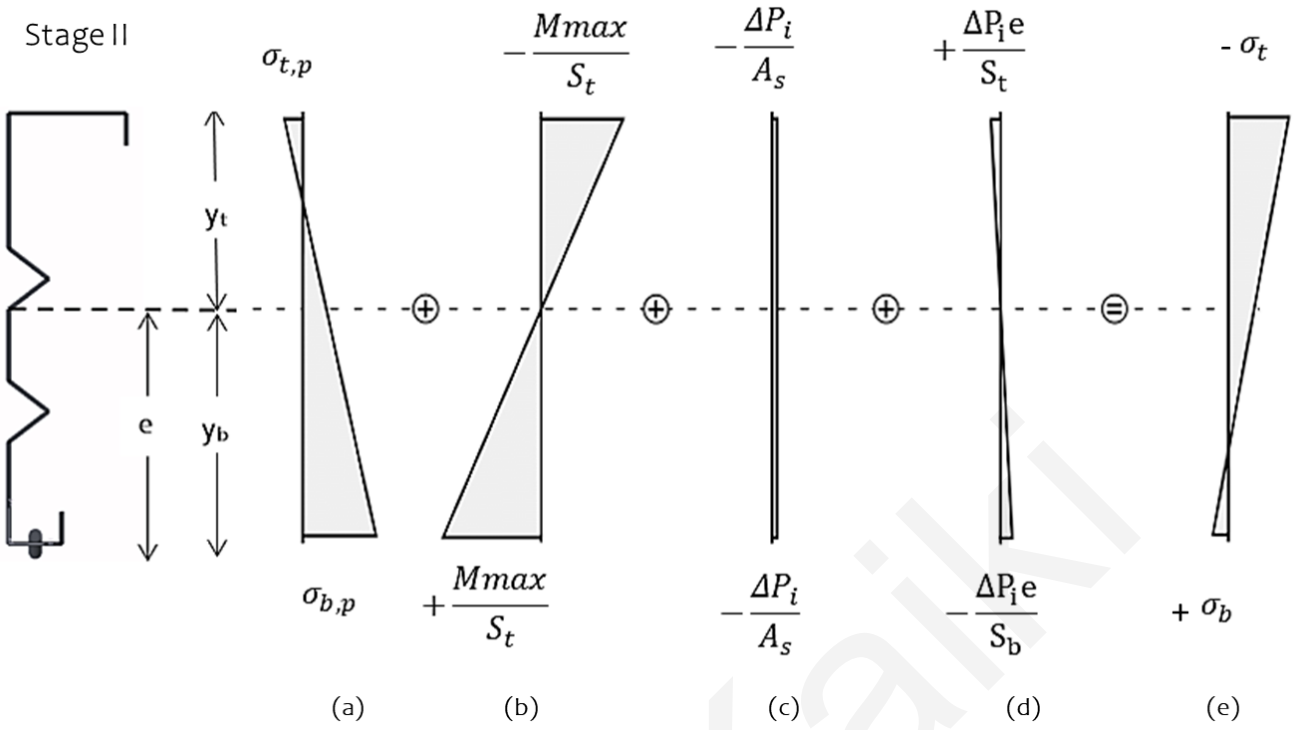

Figure 3.4: Axial stress distribution at the critical cross-section at the end of Stage II. (a) Stress distribution from Stage I, (b) bending component due to Mmax, (c) uniform compression component due to ΔP, (d) bending component due to the eccentricity of ΔP, and (e) net axial stress distribution.

The expressions for the net stress levels in the upper σt and lower σb end fibres of the cold formed steel section at the end of Stage II can be obtained as follows:

$$\sigma_{t,p} = (Pi + \Delta P)\left(\frac{e}{St} - \frac{1}{As}\right) - \frac{Mmax}{S_t}, \tag{3.4}$$

$$\sigma_{b,p} = -(Pi + \Delta P)\left(\frac{e}{Sb} + \frac{1}{As}\right) + \frac{Mmax}{S_b}, \tag{3.5}$$

The strength of the prestressed member in stage II is affected either by the limiting strength of the steel beam when subjected to vertical loading or by the tensile strength of the cable when subjected to both Pi and ΔP. As shown in Figure 3.4 (e), the capacity of the cross-section in Stage II is limited by the compression level within the top flange with failure occurring either by local/distortional buckling or by yielding, depending on the thinness of the cross-section.

The vertical deformations caused by the imposed vertical loading counteract the deflection caused in stage I. The total vertical deflection at the mid-span δII at the end of Stage II results from the superposition of the deflection induced in Stage I, as given in Equation (3.3), and the deflection due to the imposed vertical loading and the increased prestressing force from Stage II, such that:

$$\delta^{II}{}_{mid} = \left(\frac{5L^2}{48E_sI_s}\right)Mmax - \left(\frac{L^2}{8E_sI_s}\right)(P_i + \Delta P)e, \tag{3.6}$$

3.5 Concluding remarks

In this chapter, the conceptual development of prestressed cold-formed steel beams was presented. In the proposed system, a cable is housed through the bottom flange of the cold-formed steel beam in an eccentric position from the strong geometric axis, anchored at the ends of the beam and is free to elongate along the length of the member. The beam is held laterally so as to prevent torsional buckling.

In addition, the two loading stages to which the proposed system is subjected were presented. Stage I is the prestressing application stage and stage II involves the application of vertical loading. Then, the distribution of axial stresses in the critical cross-section of the prestressed members was studied, and linear elastic analytical expressions were developed to describe the mechanical behavior of the system during the two loading stages.

Chapter 4 – Finite Element Modeling

4.1 Introduction

This chapter presents the main characteristics of the FE models used to simulate the mechanical behavior of the proposed system. The FE modeling idealizes the material response, the beam-cable connection, and the loading boundary conditions.

The developed FE models are used to study the behavior of the proposed beams during different loading stages, investigate the effect of key control parameters, and evaluate the suitability of the developed design recommendations.

4.2 Development of finite element models

The FE modeling of the system is performed by the commercial FE analysis package ABAQUS (2019), which has been widely used in previous research for cold-forming modeling of steel members (Young, B. and Yan, J., 2004; Dinis, P. B. et al. 2007; Kyvelou, P. et al., 2018)

Nonlinear analysis of geometric and material defects is implemented to understand the mechanical behavior of cold-formed prestressed steel beams and to provide a complete picture of the scale of the potential benefits that can be obtained from prestressing.

4.2.1 Element types

The S4R shell element was used to model the cold-formed steel beam. ABAQUS shell elements allow the modeling of curved, intersecting shells that can exhibit non-linear material response and undergo large total displacements and rotations. They are commonly used to model thin-walled structures where one dimension (i.e., thickness) is significantly smaller than the other dimensions, as they can accurately capture local instability phenomena such as local and distortional buckling.

For the given simulation, the linear S4R 4-node shell element with reduced integration and hourglass control (ABAQUS, 2019) was used to model the beam.

In general, the S4R element is a three-dimensional, doubly curved four-node shell element with six degrees of freedom per node using bilinear interpolation and reduced integration. S4R reduced integration elements are computationally more efficient than the equivalent S4 full integration elements. This is due to the fact that, in the first case, there is only one integration point in the plane per element, whereas, in the second case, there are four integration points.

The prestressing cable was modeled with three-dimensional T3D2 truss elements, which can only carry axial forces. The T3D2 elements have a rectilinear profile with an integration point at the center and use linear interpolation between the two end nodes to determine the displacement field. The axial stress along the element is constant.

4.2.2 Meshing scheme

The density of the mesh plays a crucial role in the ultimate load and collapse response of cold-formed steel elements subjected to local, distortional and/or global buckling (Schafer, B. W. et al., 2010) To this end, a mesh sensitivity analysis was conducted to determine a suitable cross-sectional discretization that would be both accurate and computationally inexpensive.

A uniform grid was selected throughout the cross-section, with the longitudinal element for both the cold-formed steel beam and the cable being up to 5 mm. Particular emphasis was placed on the bottom flange where the openings are located, so that the mesh elements maintain their rectangular shape. Otherwise, variations in the final response of the system would be created. A finer mesh (Figure 4.1) was placed around the openings for better response results for both the beam and the cable.

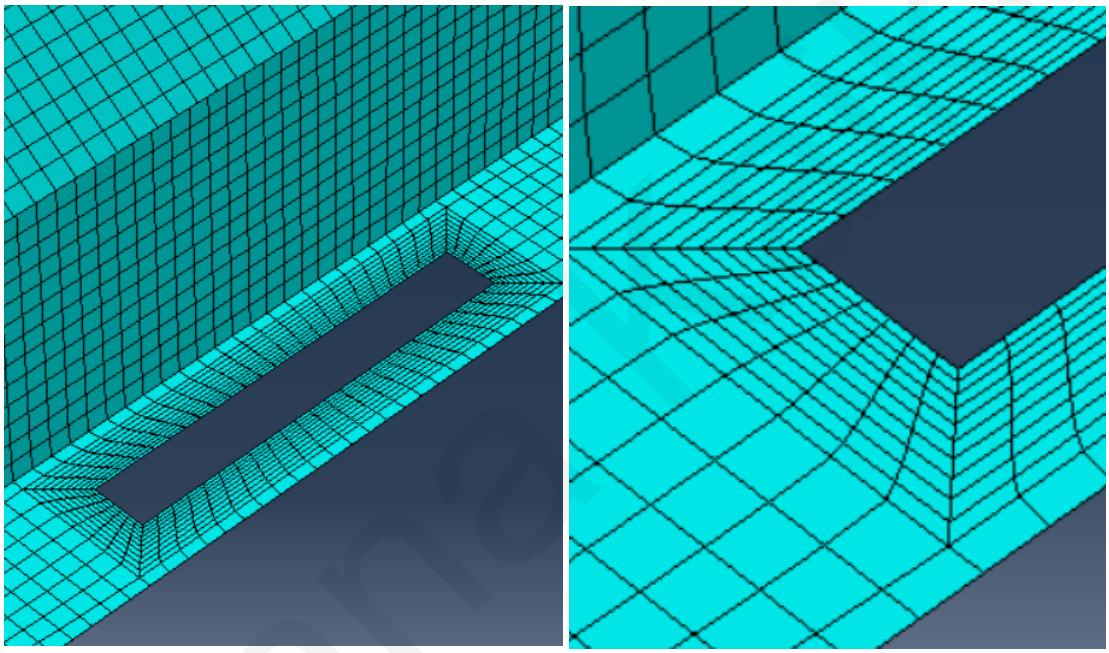

Figure 4.1: Finer mesh around the openings of the bottom flange

4.2.3 Material modelling

The behavior of the cold-formed steel beam material and the high-strength steel cable was modelled in ABAQUS. In order to account for the changes in cross-section due to deformation, the mechanical constitutive responses were converted to true stress σ_{true} and logarithmic plastic deformation ϵ_{ln}^{pl} using the following functions:

$$\sigma_{true} = \sigma\,(1+\epsilon) \tag{4.1}$$

$$\epsilon_{ln}^{pl} = \ln(1+\epsilon) - \frac{\sigma_{true}}{E} \tag{4.2}$$

where σ and σ are the mechanical stress and strain respectively, and E is Young's modulus of elasticity.

The above transformation was also necessary in the case of the cable, since, by definition, the elements of the network have a Poisson's ratio equal to 0.5 and are therefore considered to be made of incompressible material (i.e. their volume does not change under deformation).

4.2.3.1 Cold-formed steel

The main material characteristics of cold-formed steel were discussed in Section 2.3.2. For the purpose of this work, two different material models were used, the elastic perfect-plastic and the Ramberg-Osgood model.

(a) Elastic, perfect plastic

Cold-formed steel typically features a rounded, non-linear material response with strain hardening and no discrete yield point, as shown in Figure 2.9 (a). In order to enable a comparison of the FE models, the material behavior was idealized by considering elastic, perfect-plastic material response without strain hardening.

It was adopted, yield stress $F_{y,s}$=491 N/mm^2 and Young's modulus E_s=201 kN/mm^2, based on the experimental work conducted by Kyvelou, P. et al., (2018).

It is noted that, the residual stresses and strength increase in the angular regions resulting from the plastic deformations induced during the cold forming process were not modelled in conjunction with this material model.

(b) Ramberg-Osgood

For a more realistic modelling of the cold formed steel material behavior, the two-stage Ramberg-Osgood model was used. This model provides the possibility of direct comparison of FE results of the load-carrying capacity estimates, which are based on the empirical direct strength method. It was originally developed by Ramberg and Osgood (1943) to capture the nonlinear response of metallic materials such as aluminium and stainless steel. Subsequently, this model was modified by Mirambell and Real, (2000) and Rasmussen (2003) until Gardner and Ashraf (2006) proposed the following expressions:

$$\epsilon = \frac{\sigma}{E_s} + 0.002\left(\frac{\sigma}{\sigma_{0.2}}\right)^{n} \quad \text{for } \sigma \leq \sigma_{0.2}, \tag{4.3}$$

$$\epsilon = \frac{\sigma - \sigma_{0.2}}{E_{0.2}} + \left(\epsilon_{t0.1} - \epsilon_{t0.2} - \frac{\sigma_{1.0} - \sigma_{0.2}}{E_{0.2}}\right)\left(\frac{\sigma - \sigma_{0.2}}{\sigma_{1.0} - \sigma_{0.2}}\right)^{n'_{0.2,1.0}} + \epsilon_{t0.2}$$

$$\text{for } \sigma > \sigma_{0.2}, \tag{4.4}$$

where $E_{0.2}$ is the tangent modulus at the 0.2% proof stress $\sigma_{0.2}$, which is typically taken as the equivalent yield point for design. Moreover, $t_{0.2}$ and t1.0 are the total strains at 0.2% proof stress $\sigma_{0.2}$ and 1.0% proof stress σ1.0 respectively

The rounding of the first and second stage of the constitutive relationship is defined by the hardening stress exponents n' and $n'_{0.2,1.0}$ respectively. Regarding the determination of the 1.0% proof stress, Haidarali and Nethercot (2011) utilized experimental data from tensile coupon tests conducted by ; 2006) to propose the following expression, where $\sigma_{0.2}$ and $\sigma_{1.0}$ are in N/mm^2

The modified two-stage Ramberg-Osgood model has been used in extensive research (Haidarali and Nethercot. 2011; Kyvelou et al. 2018) to accurately reproduce the nonlinear material response of cold-formed steel structural elements.

Following the same approach as Kyvelou et al. (2018) residual stresses through the cross-sectional thickness of the cold-formed steel were not introduced in the FE models of this study, since their effect is considered to be inherently included in the constitutive relationships derived from the tensile coupon tests, as discussed in Section 2.3.2.3.

4.2.3.2 High-strength steel cable

The high-strength steel cable was modeled as elastic, perfect plastic, and the plastic part of the material curve determines the leakage of the cable.

The cable yield stress was defined as $F_{y,c}$=1860 N/mm^2 according to Gosaye et al. (2014) while the Young's modulus was obtained E_c=195 kN/mm^2 based on clause 3.3.6(3) of EN-1992-1-1, (2004) and the research of Madrazo-Aguirre et al.,(2015b). The FE simulation was terminated when the cable reached the yield stress. The thermal expansion coefficient of the cable α_{th} was set equal to 1.2×10^{-5} K^{-1} according to 3.3(1) of EN-1993-1-3, (2006). Through this coefficient, the in-cable prestressing force is applied to the FE models.

4.2.4 Beam–cable connection

An idealized connection between the cold-formed steel beam and the cable was modeled by making the following assumptions:

(i) The cable is unconnected and concentric with respect to the bottom hollow flange of the cross-section along the entire length of the beam opening.

(ii) The end anchorages are the only locations where there is a connection between the beam and the cable.

(iv) The cable is angled to pass through the openings.

(iii) There is no loss of prestressing within the cable or at the anchors.

Through ABAQUS (2019), two types of constraints were imposed:

Coupling was applied, to model the anchorage, through the cable start node to a node of the bottom leg of the beam binding all degrees of freedom (DOF) and correspondingly held for the end nodes. This type of connection ensured uniform transfer of the prestressing force across the entire bottom flange at both ends of the beam and thus prevented excessive stress concentrations and consequently local failures.

In addition, two sets of linear constraint equations, modelled with the keyword *****Equation in ABAQUS (2019), were defined, introduced along the cable and the steel beam corner nodes, where it limited the vertical displacement (DOF-2) and in-plane bending (DOF-6). In this way, the cable was kept in the center of the bottom flange, but was allowed to elongate freely along the member since DOF-1 remained unconstrained.

4.2.5 Boundary Conditions

To model the simply supported boundary conditions at the two end supports, kinematic coupling constraints were applied to link the DOFs of the end nodes of the member to those of a single reference point, which was defined at the centroid of the cross-section. At the left reference point, its vertical (DOF-2) and out-of-plane (DOF-3) displacements were constrained, while only the vertical (DOF-2) displacements were constrained at the right reference point. These constraints resulted in the effect of boundary conditions being evenly distributed throughout the cross-section. In addition, the kinematic coupling constraints lead to distortion-stable conditions at both end supports.

In addition, longitudinal rigid body motion of the member was prevented by limiting the longitudinal (DOF-1) displacement of the central node of the truss at mid-span. Finally, at intervals of 600 mm along the length of the member, out-of-plane (DOF-3) displacements were limited and thus the member is considered to be fully restrained against lateral-tensional buckling.

4.2.6 Loading Conditions

Two different stages were defined to model the prestressing and the imposed vertical loading conditions.

In the first stage, the prestressing force was modeled by imposing a negative temperature change on the cable using the *****Temperature keyword (ABAQUS, 2019). The restrained thermal contraction of the cable resulted in the development of a tensile force Pi, which was then transferred as an initial prestressing force to the member anchors. The temperature difference ΔT required to induce the desired prestressing force can be calculated using the expression $Pi=-E_cA_c\alpha_{th}\Delta T$, where α_{th} is the thermal expansion coefficient of the cable, as defined in Section 4.2.3.2. The approach of introducing prestressing using thermal loading has been successfully used in previous studies (Gosaye et al., 2014) and is particularly effective for elastic materials.

In the second stage, the uniformly distributed loading was modelled by applying concentrated point loads at the junction between the top flange and the web along the entire beam.

4.2.7 Solution scheme

The first loading stage was modelled using a geometrically nonlinear 'Static' analysis (ABAQUS, 2014); in this manner, termination of the analysis when reaching the predefined initial prestress level was ensured. The second loading step was performed using the modified Riks arc-length solver (Riks, 1979) by means of a geometrically nonlinear 'Static, Riks' analysis (ABAQUS, 2014), which is typically employed to analyze complex geometrically nonlinear responses in FE models, such as in the case of cold-formed steel members (Schafer et al., 2010).

4.3 Concluding remarks

In this paper, finite element (FE) was used to simulate the mechanical behavior of the proposed system. In this chapter, the main features of the FE models were firstly presented. In summary, shell and mesh elements were used to model the cold-formed steel and the cable respectively, and a sufficiently fine mesh was used to ensure computational accuracy and efficiency. The cold-formed steel modeling was implemented considering, elastic, perfect plastic and Ramberg-Osgood model. The cable was modeled using elastic, perfect plastic material model. The characteristics of these disturbances were based on the critical buckling modes of the member, which were derived using CUFSM software and Buckle Analysis from ABAQUS.

Kinematic coupling, equation constraints and lateral constraints were used to model the beam-cable connection, boundary conditions and loading conditions.

Chapter 5 – Mechanical Behavior & Parametric Studies

5.1 Introduction

In the first section of this chapter, the FE results for bare beam, un-prestressed beam with cable and fully prestressed beam developed are presented and compared. The purpose of this chapter is to gain an in-depth understanding of the effect of prestressing on the behavior of the members under study. Thus, the moment-strain responses and deformed modes of the system are analyzed in detail. In this way, the origin of the advantages obtained in terms of load-bearing capacity and functional performance of the prestressed members is demonstrated.

The main advantage of numerical models over experimental investigations is that several simulations can be performed in parallel, thus offering significant advantages in terms of cost and time. This is exploited in the second section of this chapter where the influence of key control parameters on the behavior of the proposed prestressed system is investigated. A series of parametric studies is thus carried out, where the control parameter under study is varied while the others remain constant. The control parameters studied here were the cable size and the number of openings. These results are used to determine how to maximize the achieved benefits, demonstrating significant improvements in the structural performance of cold-formed steels.

5.2 General

The FE results were obtained using the modeling approach presented in Section 4.2 and were obtained using the elastic, perfectly plastic material model presented extensively in Section 4.2.3.1(a). The FE sample results were based on the geometry shown in Figure 3.1, with the dimensions listed in Table 3.1. Additional geometric properties of the reference beam are given in Table 5.1.

P_{max}	267 kN	e	159 mm
A_s	1661 mm^2	S_b	128315 mm^4
I_s	22294762 mm^4	S_t	147403 mm^4
A_c	78.5 mm2		

Table 5.1: Properties of the cold-formed steel reference beam and cable.

The following cases are considered in this section:

i. Bare cold-formed steel beam
ii. Non-prestressed beam in the presence of cable
iii. Fully prestressed beam

Based on the CUFSM and cFSM results, presented in Table 5.1. the Pmax can be calculated to be 266.97 kN in the case of the reference beam. It is noted that in the FE models in this section, the length of the beam is 4800 mm.

5.2.1 Moment–deflection responses

First a comparison is made between the FE results for linear and non-linear material with the theoretical results obtained using CUFSM. The applied load in stage II can be expressed in terms of M_{max} (i.e. the maximum moment due to the applied load). In addition, the overall system response can be measured in terms of the vertical deflection of the beam at mid-span δ_{mid}. The response M_{max} versus δ_{mid} of the system is presented for three model cases, taking into account FE results and theoretical results. A comparison between linear and nonlinear models is also made, keeping the ideal geometry. The theoretical results were calculated using equations (3.3) and (3.6) for Stages I and II respectively.

In Figure 5.1 below, a comparison between the FE results for linear and non-linear material with the theoretical results is made, where moderate agreement is observed. This discrepancy is most likely due to two main reasons. Firstly, pre-stress is not taken into account when calculating the theoretical values and secondly, initial geometric imperfections are absent in the FE models.

The effect of imperfections as well as non-linearity is a decisive factor for the structure, as they cause early development of local and/or distortional buckling during loading. In addition, they are accompanied by a gradual decrease in flexural stiffness and reduced limit moment capacity of the beams, as shown in Figure 5.2.

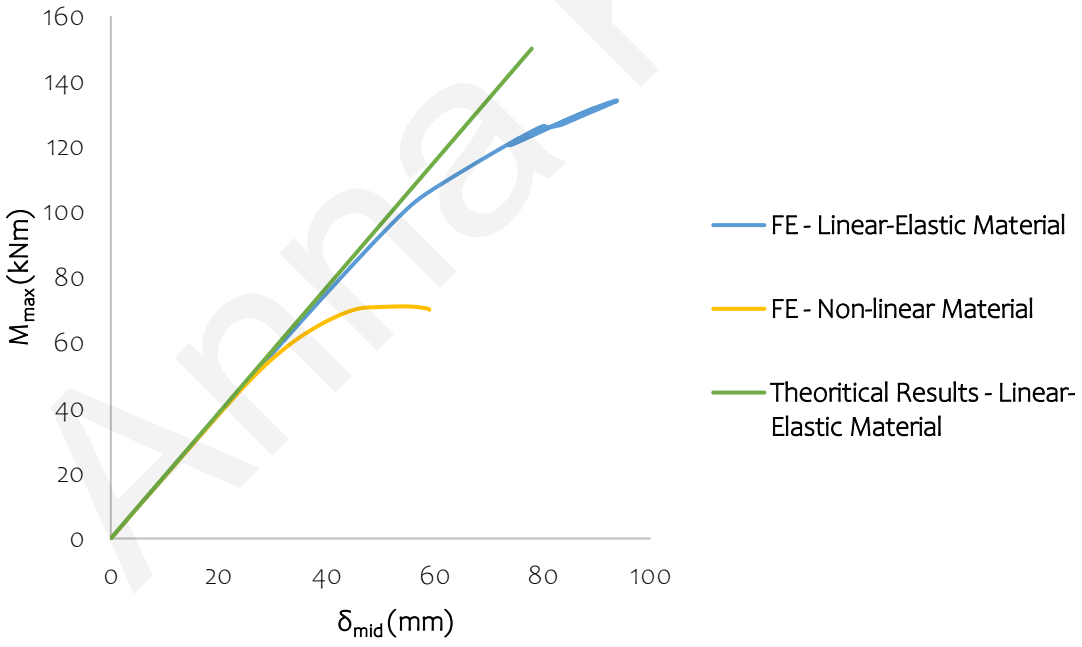

(a)

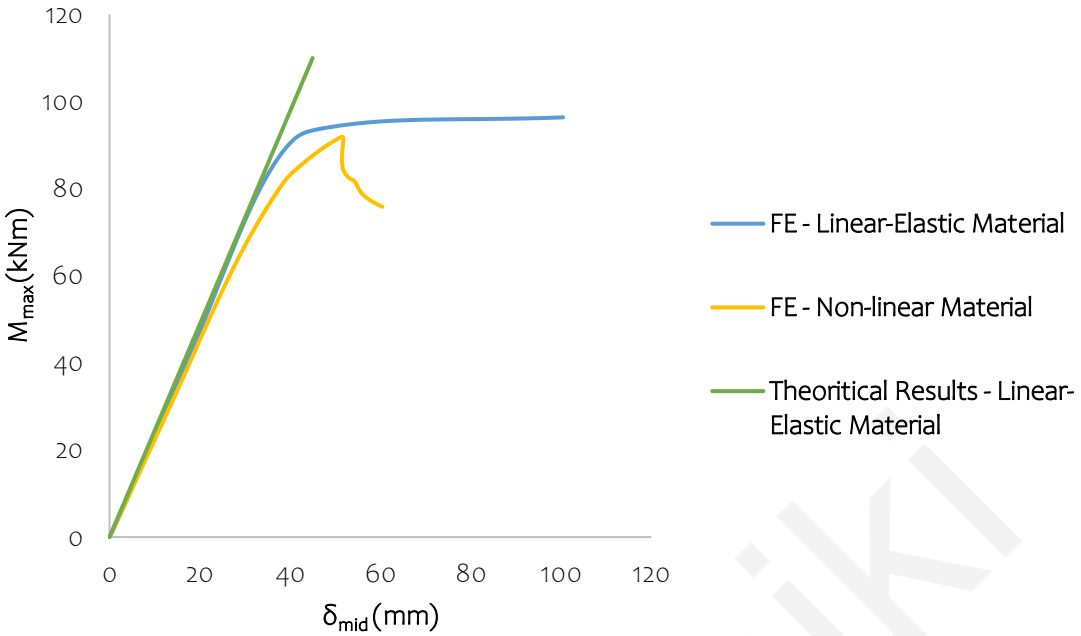

(b)

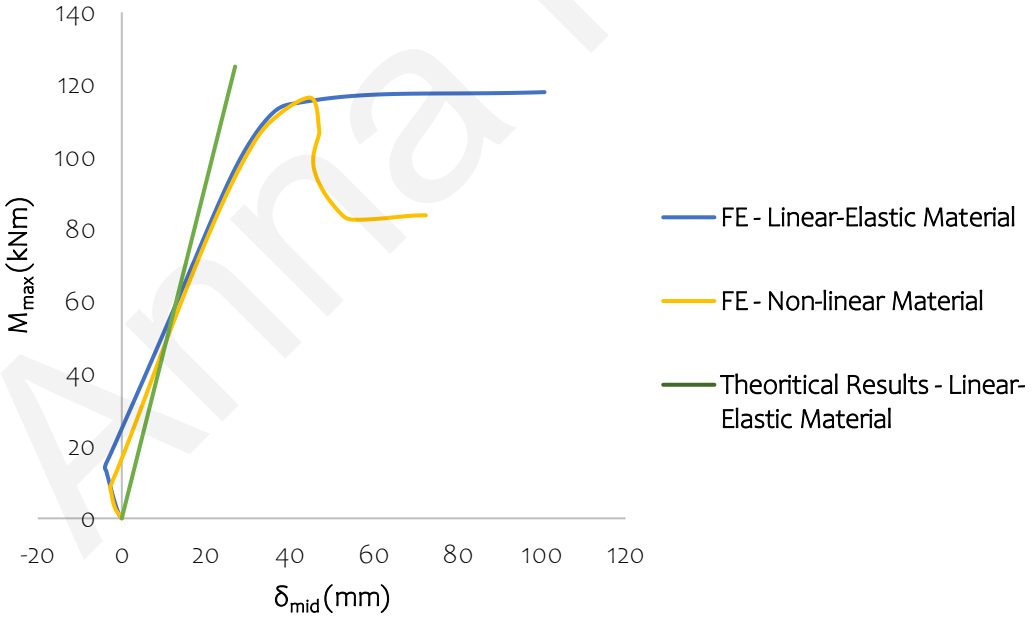

(c)

Figure 5.1: Comparison of the normalized torque-strain response of the three sample FE models with the theoretical results. The FE results correspond to the linear-elastic and non-linear material model for (a) bare cold-formed steel beam, (b) non-prestressed beam in the presence of cable and (c) fully prestressed beam. The theoretical results are for linear material.

Proof of the decisive role of non-linearity is shown in Figure 5.2. More specifically, in the case of the bare beam with linear-elastic material behavior (Figure 5.2(a)), the maximum moment is equal to 134kNmm, while with non-linear material behavior, the maximum moment is equal to 71kNmm, i.e. a 47% reduction. In the case of the beam with non-prestressed cable with linear-elastic material (Figure 5.2(a)), the maximum moment is equal to 102kNmm while in the case of non-linear material, the maximum moment is equal to 91kNmm, i.e., a reduction of 11%. Finally, in the case of the prestressed cable beam with linear-elastic material (Figure 5.2(c)), the maximum moment is equal to 128kNmm while in the case of non-linear material, the maximum moment is equal to 115kNmm, a reduction of 11%.

Therefore, it is easy to see that the non-linear material has reduced strength and stiffness compared to the linear material, since the maximum moment that the structure can receive is significantly lower than that of the elastic material.

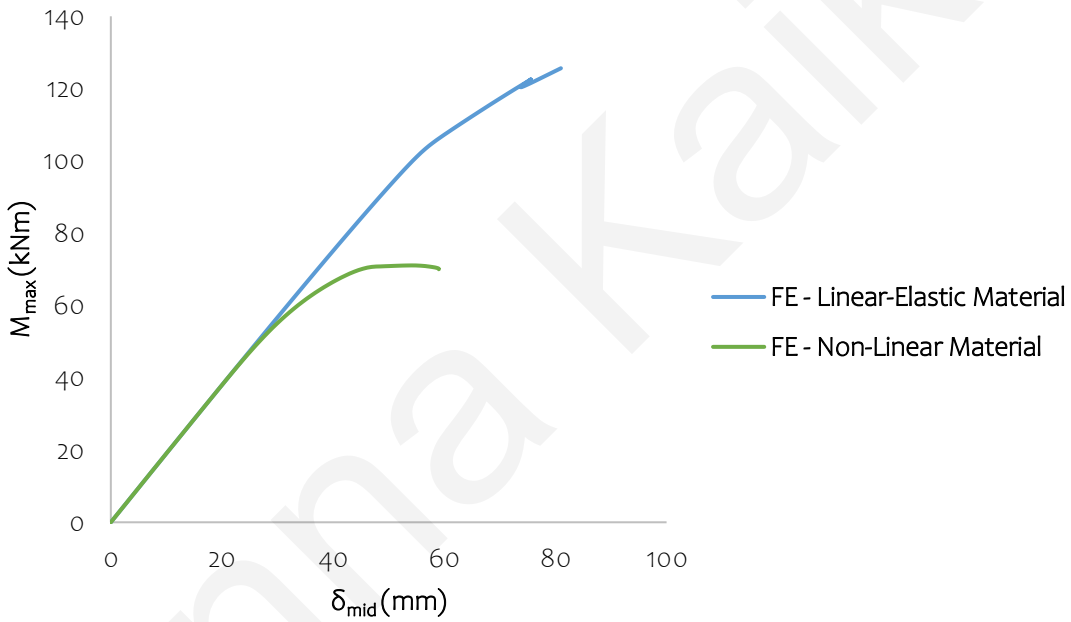

(a)

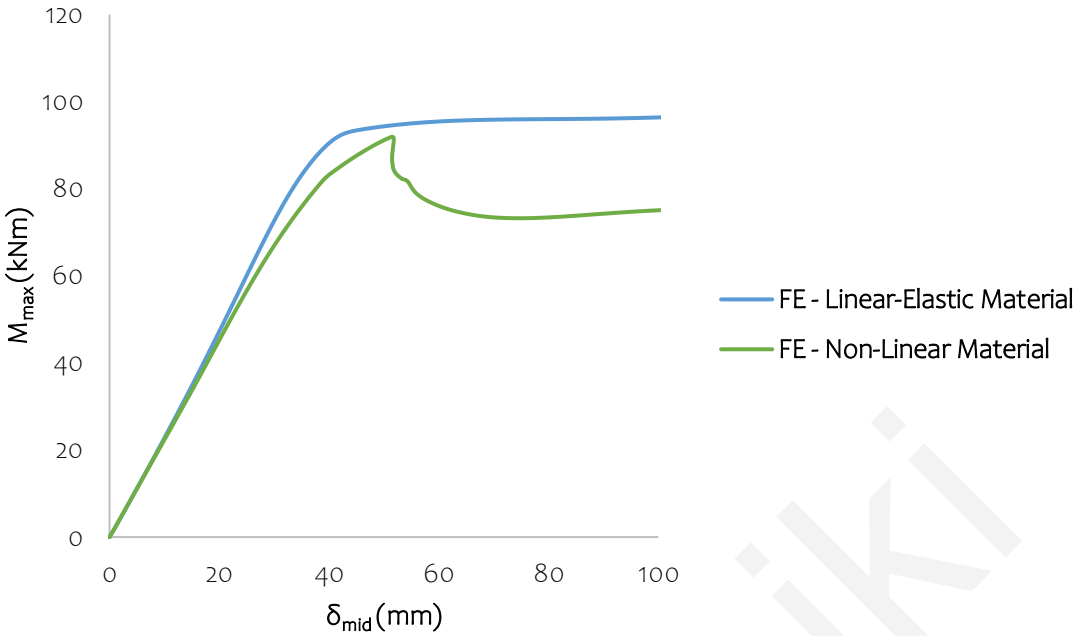

(b)

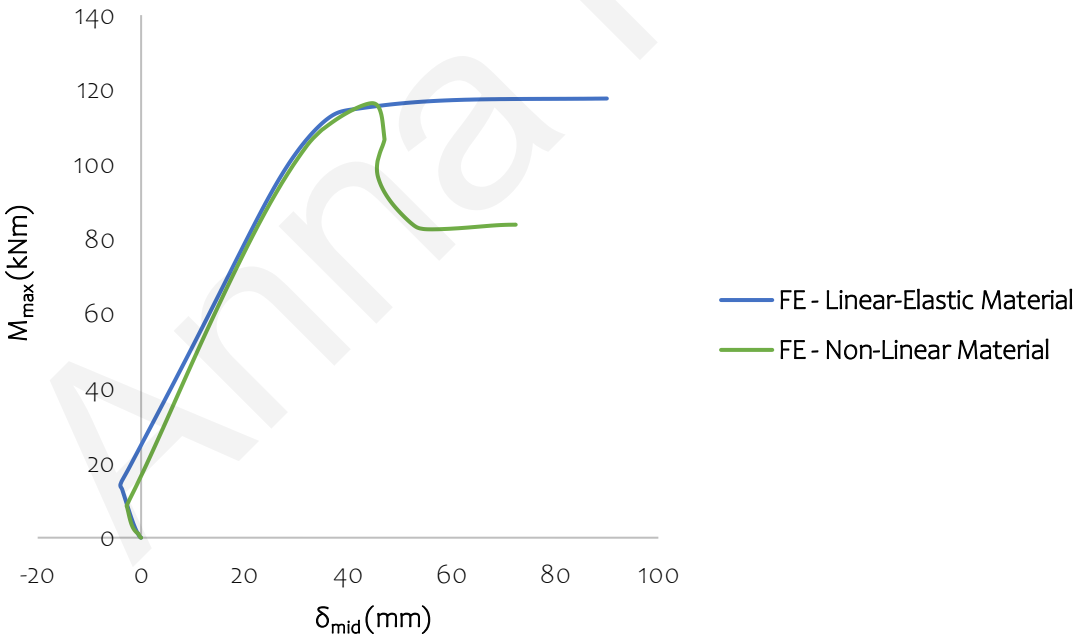

(c)

Figure 5.2: Comparison of the normalized moment-strain response of the three FE models with linear-elastic material and non-linear material. The FE results correspond to (a) bare cold-formed steel beam, (b) unprestressed beam in the presence of cable and (c) fully prestressed beam.

A comparison is made between the three models bare beam, non-prestressed beam and fully prestressed beam with linear material first and then with non-linear material. From Figures 5.3-5.4, it is observed that the moment capacity of the prestressed beam $M_{ult,p}$ is significantly higher than that of the bare beam M_{ult} both in the case of beams with linear-elastic material and in the case of beams with non-linear material. This increase represents the main benefit of the prestressing process in terms of the load-bearing capacity of the beam.

More specifically, in Figure 5.3, comparing the bare beam with the non-prestressed cable and the prestressed beam, a 23% increase in strength is observed. The material was linear-elastic, the initial prestressing force was equal to 266.96 kN and the radius of the cable was equal to 5 mm.

Furthermore, in terms of vertical deformations of the beam, the application of the prestressing caused an initial deformation in the middle of the span, shifting the moment-deformation response to the left. For the case of the beam with linearly elastic material, a reduction of 11% was achieved. Finally, by comparing the slopes of the bare steel and unprestressed responses, it is also observed that the introduction of the cable increases the stiffness of the system, thus reducing the deformations of the beam.

In Figure 5.4, by first comparing the bare steel beam with the non-prestressed beam with cable and the prestressed beam there was an increase in strength of 28% and then comparing the bare beam with the prestressed beam there was an increase in strength of 67%. The material was non-linear. The reduction in vertical deformation is more pronounced in the case of the non-linear material at a rate of 32%.

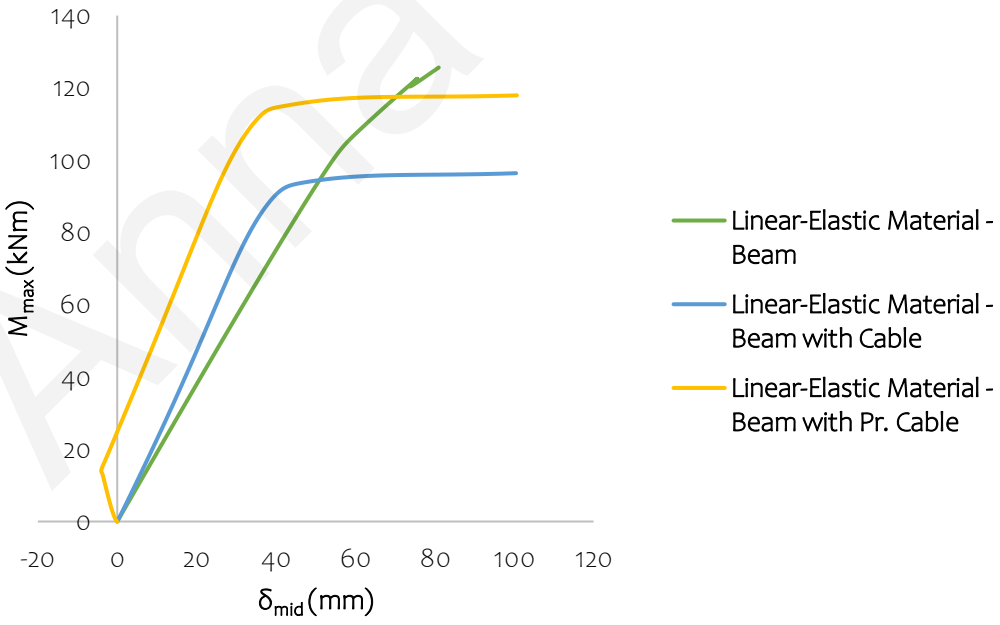

Figure 5.3: Comparison of the normalized moment–deflection response of the three samples FE models for (a) Bare cold-formed steel beam, (b) Non-prestressed beam in the presence of cable, and (c) Fully prestressed beam. The FE results correspond to the linear material model.

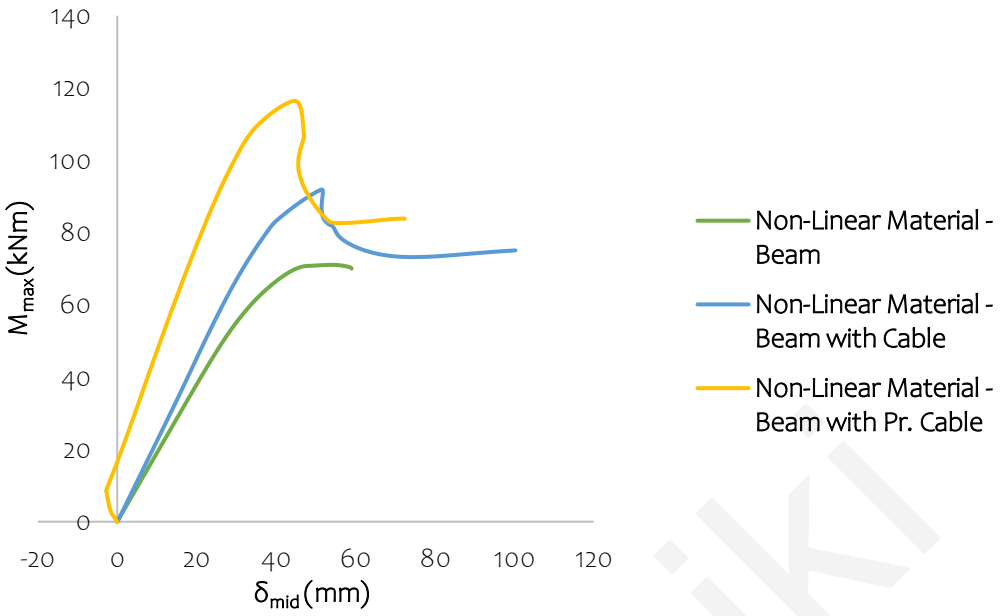

Figure 5.4: Comparison of the normalized moment–deflection response of the three samples FE models for (a) Bare cold-formed steel beam, (b) Non-prestressed beam in the presence of cable, and (c) Fully prestressed beam. The FE results correspond to the non-linear material model.

As discussed in Section 3.4.3, due to the unconnected nature of the beam cable, the cable does not fully contribute to the flexural stiffness of the system. Therefore, the increase in the flexural stiffness of the beam due to the presence of the cable was calculated by considering the effect of ΔP on the moment-deformation response, as given in equation (3.6).

Depending on the initial prestressing force and the ductility of the cold-formed beam steel, prestressing can delay local/distortional buckling and thus prolong the full utilization of the flexural stiffness of the cross-section. This is because the initial stresses introduced during prestressing must first be overcome before the elastic buckling stress of the cross-section is reached. Consequently, the addition of the prestressed cable can potentially reduce the vertical deformation of the cold-formed steel beam during operation.

5.2.2 Deformed Shapes

The effect of prestressing is further studied by presenting the deformed shape of the fully prestressed beam at different loading stages. Figure 5.6 illustrates the three-dimensional FE representations where the indicated loading levels correspond to points A-E in the moment-deformation response of Figure 5.5.

The initial deformation at point A gradually decreases with the application of vertical loading until the unloaded position is reached approximately at point C. Finally, at point E, failure of the cold-formed steel beam occurs due to deformable buckling and then the system behavior becomes strongly unstable. In general, it is observed that, due to the initial pre-bending and the contribution of the cable to the flexural stiffness of the system, the overall

deformations of the beam are significantly reduced and thus the operational performance of the system is improved.

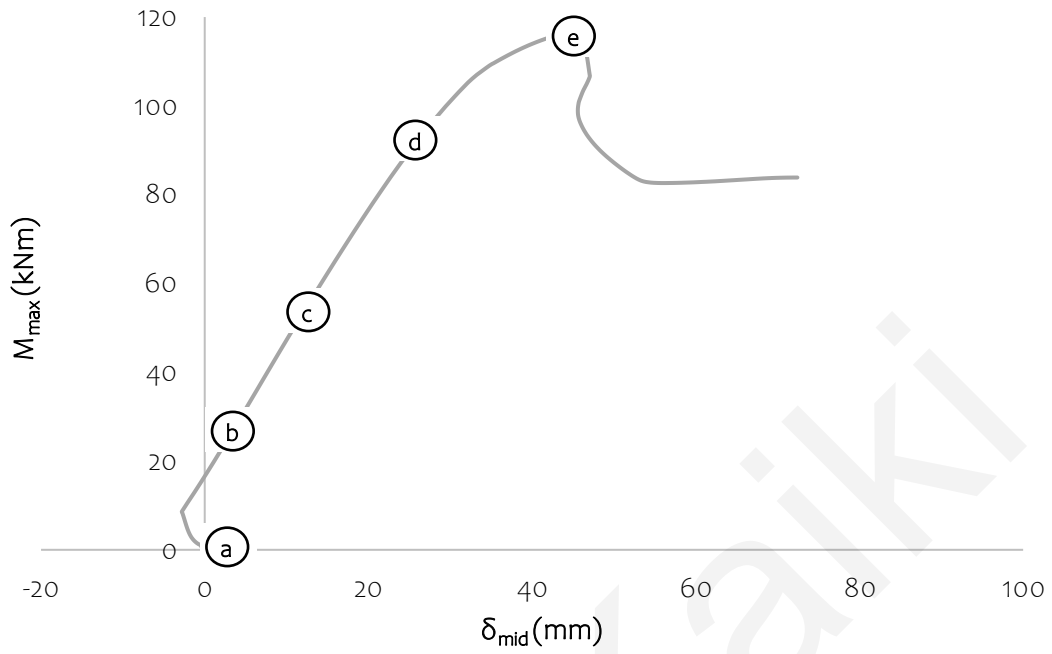

Figure 5.5: Normalized moment–deflection responses of the fully prestressed FE models. Points A–E correspond to the points in Figures 5.6.

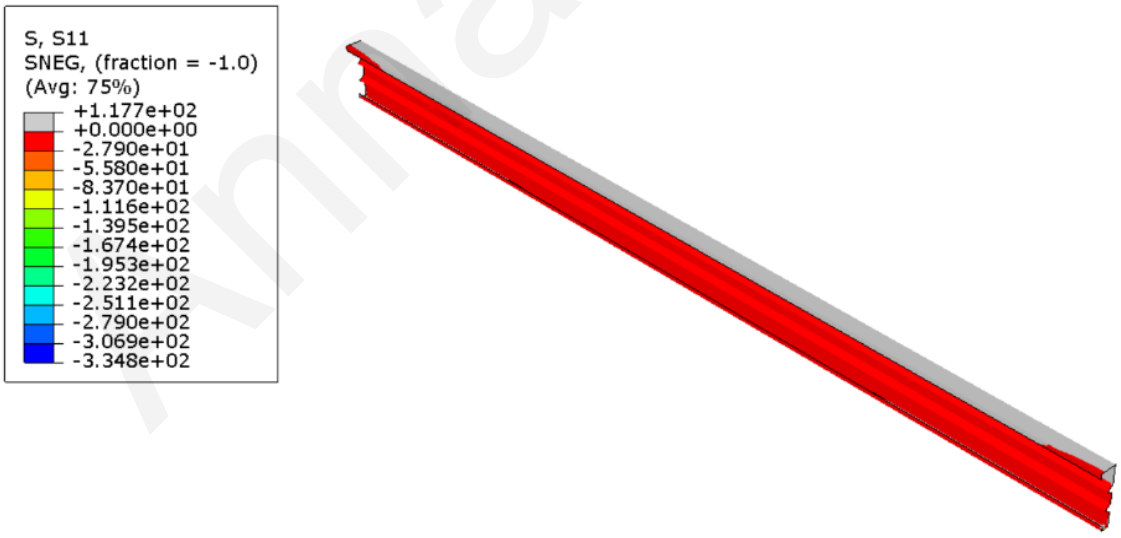

(a)

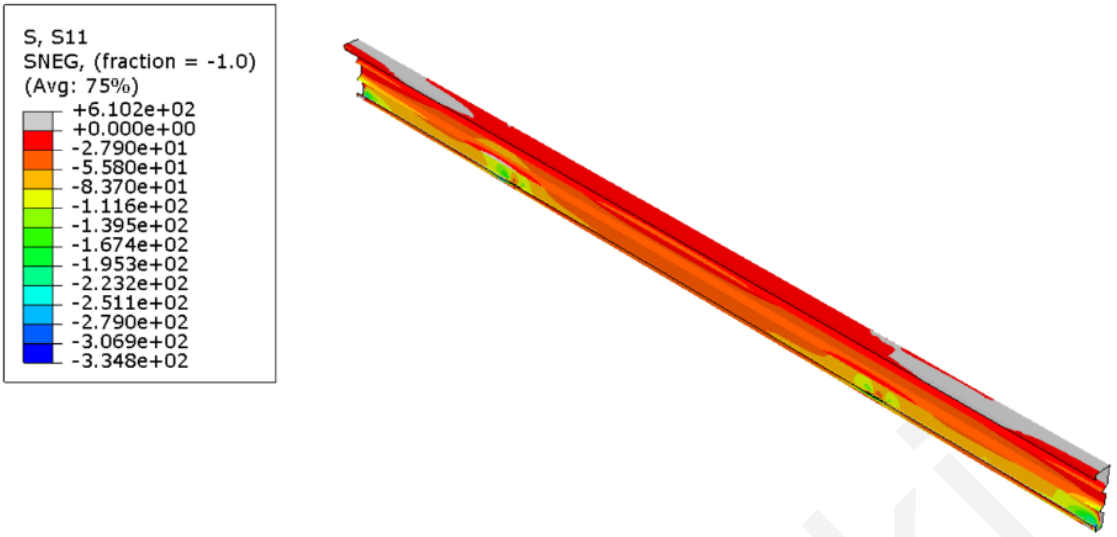

(b)

(c)

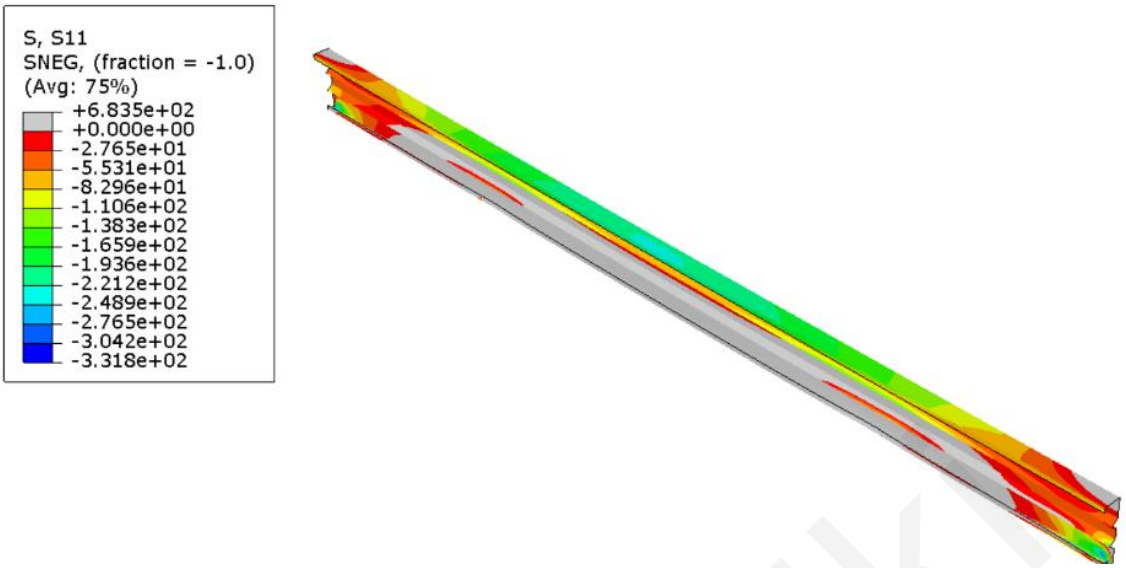

(d)

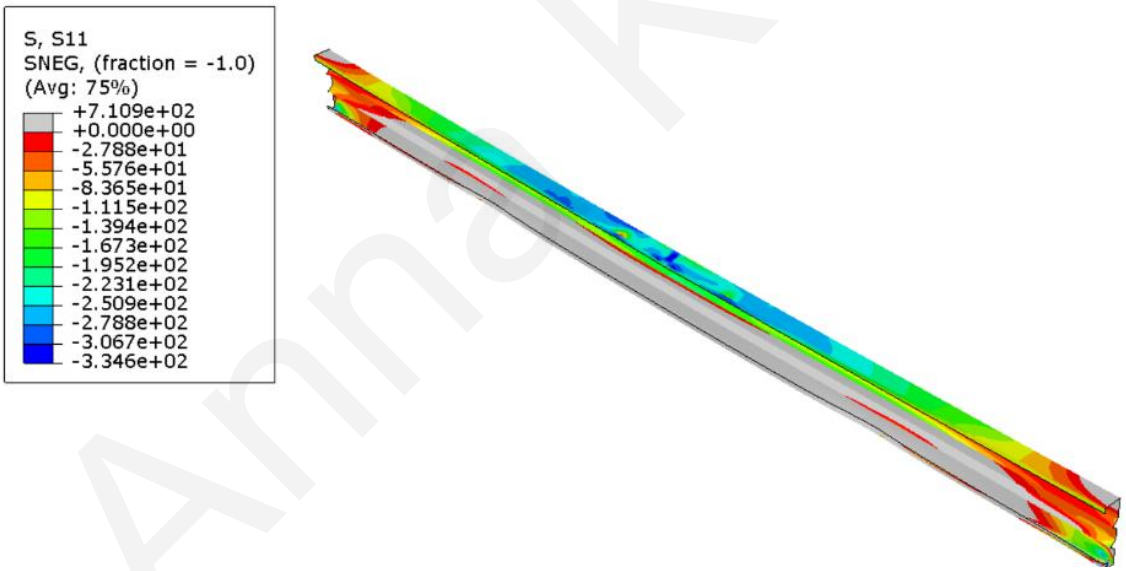

(e)

Figure 5.6: Structural behavior of the fully prestressed beam at the loading levels corresponding to Points a–e.

5.2.3 Failure modes

Failure of the proposed prestressed system occurs when the bearing capacity of either the girder or the cable is exceeded at either of the two loading stages.

In Stage I, compressive stresses develop in the bottom flange, but the cross-sectional geometry is resistant to local/distortional buckling in this region. Tensile stresses develop in the upper area of the beam. The presence of the prestressed cable and the lower lateral

restraints prevent distortional, lateral-torsional, and flexural buckling, as discussed in section 3.3.3.

In Stage II, the stresses resulting from the applied vertical loading neutralize the initial stresses induced due to the prestressing, and finally, the upper region of the cold-formed steel beam is subjected to compressive stresses. Failure is caused by local, distortional buckling or yielding of the material. In the beam under study, distortional buckling was the dominant failure mode, as shown by material yielding (dark gray) in the upper regions of the beam.

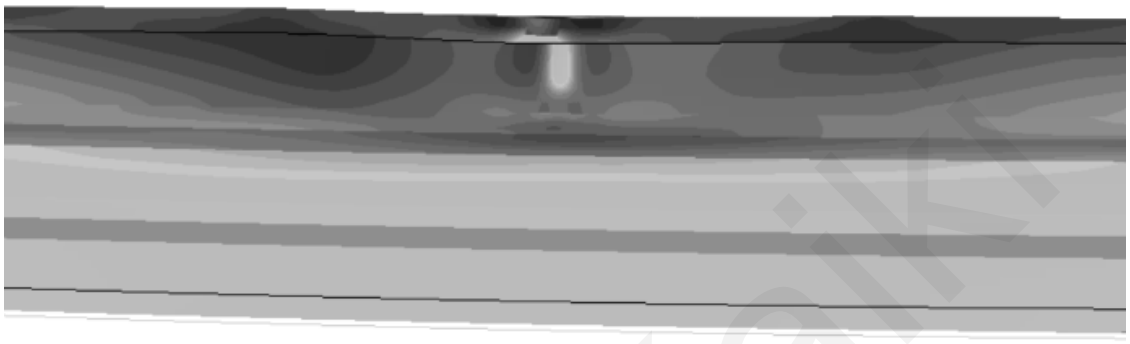

Figure 5.7: 3-D FE representation of the distortional buckling failure mode and yielded regions (dark grey) at the midspan of the fully prestressed beam just beyond the ultimate load.

5.3 Parametric studies

The purpose of the parametric finite element (FE) studies presented in this section is to investigate the effect of key control parameters on the structural performance of cold-formed prestressed steel beams. Ultimately, the results show how these parameters can be optimized and thus how the benefits of adding the prestressed cable can be maximized while minimizing the additional hardware required.

5.3.1 Basic control parameters

Parametric studies investigate the effect on the structural performance of cold-formed prestressed steel beams that have wire size and number of openings. During this investigation, the factor of interest is changed while the other characteristics of the construction remain the same.

5.3.2 Effect of Cable Size

The effect of wire size was investigated by keeping the cold steel beam geometry (i.e. profile and thickness) and initial prestressing force constant while varying the wire size. The latter was conformed using the normalized Ac/As parameter. Four wire sizes were considered according to: $A_c/A_s = \{7.0, 10.0, 14.0, 18.0\}\% \rightarrow r_c = \{6, 7.3, 8.6, 9.7\}$.

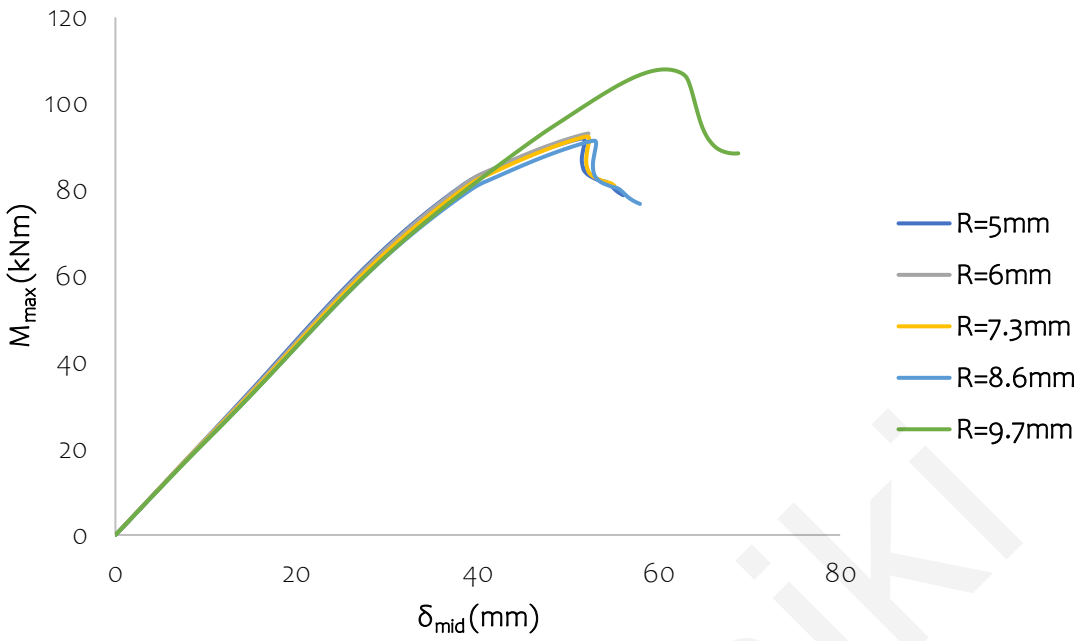

Figure 5.8: Normalized moment–deflection responses of the beam with Non-prestressed cable for different cable radius rc={6.0, 7.3, 8.6, 9.7} mm, alongside the response of the cable with rc=5mm. The FE results correspond to the non-linear material model.

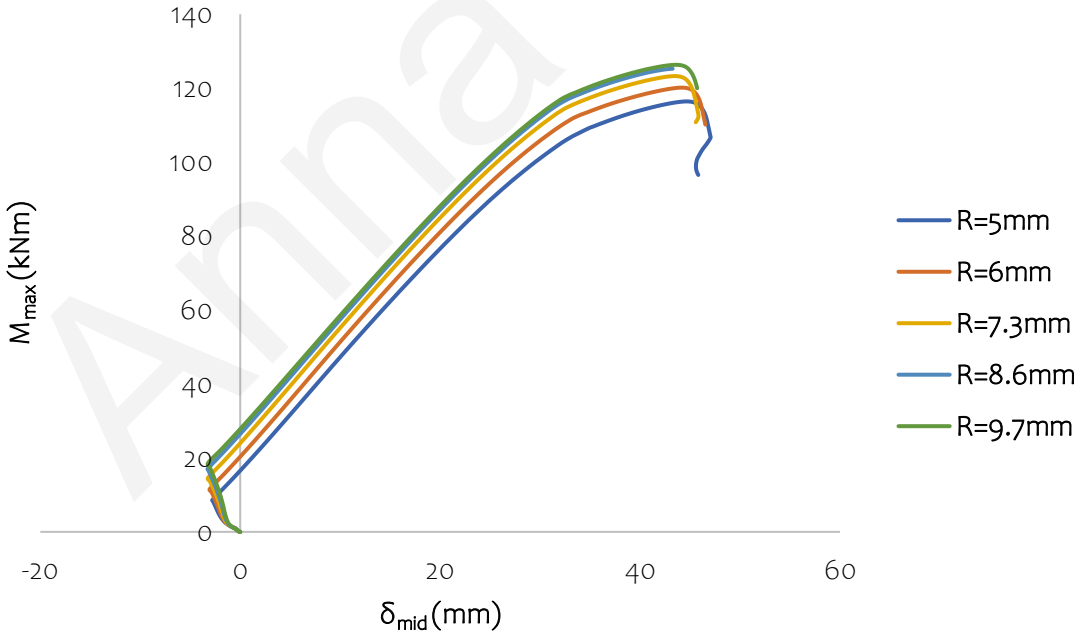

Figure 5.9: Normalized moment–deflection responses of the fully prestressed beam for different cable radius rc={6.0, 7.3, 8.6, 9.7} mm, alongside the response of the cable with rc=5mm. The FE results correspond to the non-linear material model.

As already mentioned, the addition of the prestressed cable can reduce the vertical deformation of the beam and by comparing the slopes of the bare steel and prestressed beam responses, it is observed that the introduction of the cable increases the stiffness of the system, thus reducing the deformations of the beam.

From the above diagrams, it is easy to see that in the case of beams with unstretched cable, as the radius of the cable increases, the moment capacity also increases slightly. For radii from r_c=5mm-8.6mm, the values of moment and the corresponding deformations are approximately the same. A more pronounced increase of 18% in the torque is observed between r_c=5mm and r_c=9.7mm where it increased from M_{max}=91.8kNmm to M_{max}=107.8kNmm.

In the diagram for the beam with the pre-stretched cable, the contribution to the strength is more easily seen with increasing the radius of the cable since it is progressive in the order of 2-4% between successive beams. Indicatively, comparing the values of radius r_c=5mm, M_{max}=115.9kNmm and r_c=6mm, M_{max}=119.1kNmm, an increase of 3.6% is obtained, while for the case of r_c=5mm, M_{max}=115.9kNmm and r_c=9.7mm, M_{max}=125.71kNmm, an increase of 8.4% is obtained. Therefore, increasing the radius of the cable, especially in the case of pre-stretched cable has significant benefits in increasing the strength of the system. Of course, a larger cable radius implies more material and therefore higher costs.

5.3.3 Effect of number of openings

The effect of the number of openings was investigated by keeping the geometry of the cold steel girder and cable (i.e., profile and thickness) and the initial prestressing force constant while varying the number of openings in the bottom flange of the beam. Two cases were considered. The case under study is the two openings at a distance of 2300mm and the case with 15 openings at a distance of 200mm between them.

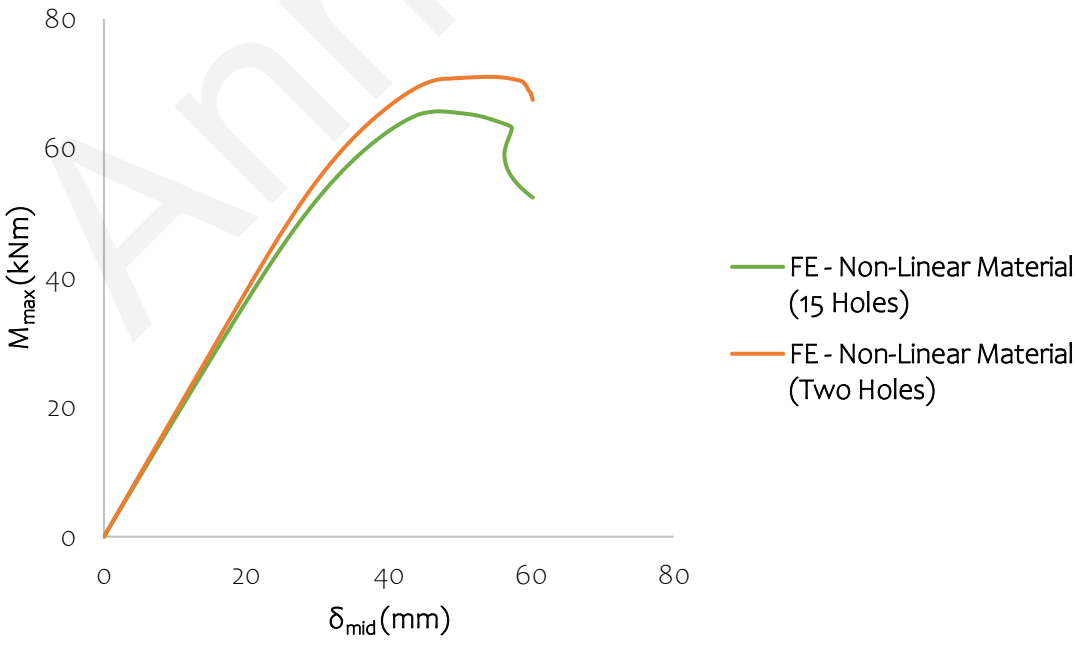

(a)

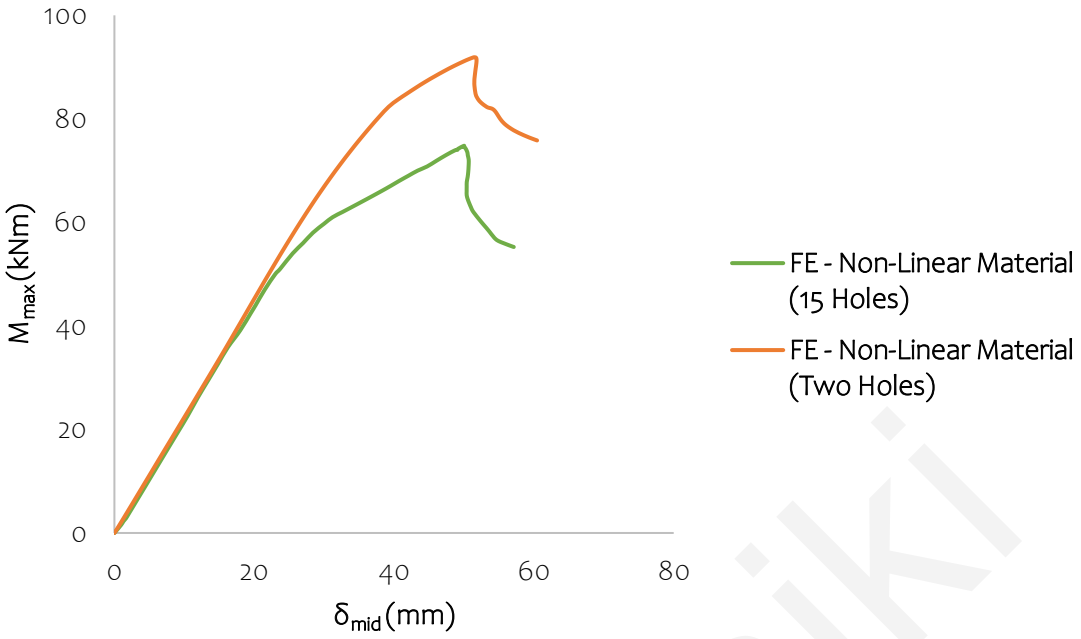

(b)

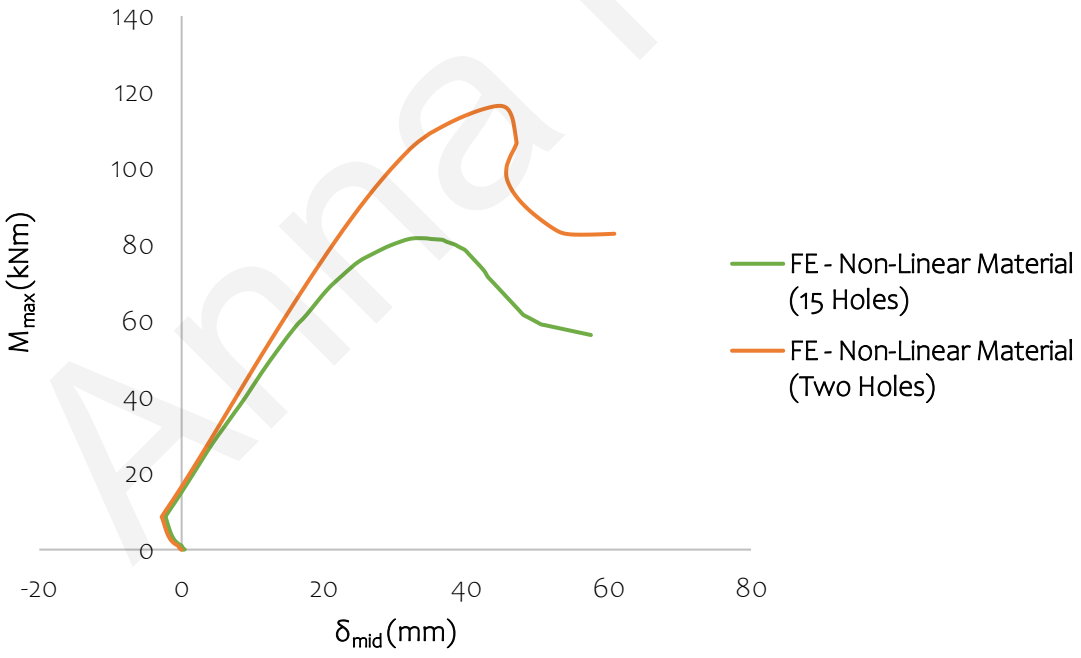

(c)

Figure 5.10: Normalized moment–deflection responses of the (a) Bare cold-formed steel beam, (b) Non-prestressed beam in the presence of cable, and (c) Fully prestressed beam with two openings against the (a) Bare cold-formed steel beam, (b) Non-prestressed beam in the presence of cable, and (c) Fully prestressed beam with many openings. The FE results correspond to the non-linear material model.

As can be seen from the above diagrams, the presence of more than two openings leads to reduced system strength. This is due to the fact that the more material there is, the more rigid the structure becomes.

In the case of single beams, the maximum moment for the beam with multiple spans equals M_{max}=65.7kNmm for δ_{mid}=47.22mm while for the beam with two spans equals M_{max}=71kNmm for δ_{mid}=54mm. A reduced moment capacity is observed for the beam with multiple openings by 7.4% compared to the beam with two openings. The maximum moment for the unprestressed cable beams with multiple spans equals M_{max}=73.4kNmm while for the beam with two spans equals M_{max}=91kNmm. A reduced moment capacity is observed for the beam with multiple openings by 19% compared to the beam with two openings. Finally, in the case of prestressed cable beams, the maximum moment for the beam with spans equals M_{max}=81.5kNmm while for the beam with two spans equals M_{max}=113kNmm. A reduced moment capacity for the beam with multiple openings is observed by 28% compared to the beam with two openings.

5.4 Concluding remarks

In this chapter, the benefits of prestressing cold-formed steel beams, in terms of enhancing strength and serviceability, have been highlighted. The proposed system includes two structural elements, the steel beam and the cable, and is subjected to combined axial compression and bending at two different loading stages. Due to the asymmetric profile of the cross-section and its thin-walled geometry, it is particularly prone to instability phenomena (buckling). For this reason, it was deemed necessary to analyze the response of the proposed members during the various stages of loading.

First, the linearity of the material is shown to be a determining factor for the strength of the structure since an increase in the stiffness and moment capacity of the beams was observed. In addition, the moment capacity of the prestressed beam is significantly greater than that of the bare beam in both the case of beams with linear elastic material and the case of beams with nonlinear material, and the vertical displacements are reduced in the case of cable prestressed beams. The latter is due to the addition of the prestressed cable which, due to its eccentric position in relation to the strong geometric axis of the beam and during prestressing, tensile stresses are caused in the upper area of the beam.

Then, the deformed shape at the critical cross-section of the beam at the various stages of loading proved to be a valuable tool for understanding the mechanical behavior and failure mechanism of the system.

Finally, a series of parametric studies were carried out, where the control parameter under study is modified while the other characteristics remain constant. The control parameters studied were the cable size and the number of openings. The parametric study on cable size made it clear that as the radius of the cable increases, so does the torque capacity while the study on the number of openings made it clear that the smaller the number of openings, the stiffer the structure. Ultimately, a well-proportioned beam and cable cross-section can provide increased structural benefits and therefore a more economical solution.

Chapter 6 – Conclusions

This Chapter is a summary of this thesis. First, the main conclusions from each Chapter are described, followed by applications of cold-formed prestressed steel members in practice.

6.1 Summary

Thanks to their high strength-to-weight ratio, cold-formed steel members provide lightweight construction solutions, offering economy in transportation and efficiency in handling, erection, and installation. However, they are particularly vulnerable to local instability due to their thin walls. These phenomena result in the full utilization of the load-carrying capacity of the cross-section.

The present work concerns an innovative concept whereby the occurrence of these instability phenomena can be delayed by means of a prestressing force to enhance the load-carrying capacity. The focus of this thesis was the conceptual development of the proposed prestressed cold-formed steel beams, which structurally and mechanically will be able to be used as a structurally efficient solution. The motivation, objectives, and methodology used are described in Chapter 1.

In Chapter 2, the basic concepts of the thesis, namely the prestressing technologies and the characteristics of cold-formed steel members, are discussed. A complete description of the technical background of the prestressing techniques used is provided. Essentially, the fundamental concept of prestressing is the introduction of stresses within structural members that are of opposite sign to the stresses induced during the applied external loading, in order to compensate for them. A literature review was then conducted, and the main findings on cold-formed steel members were presented. The manufacturing process of cold-formed steel members has a significant effect on the final behavior of the material since low temperature makes the steel stronger and more durable compared to hot-formed steel.

In Chapter 3, the conceptual development of prestressed cold-formed steel beams was presented. In the proposed beams, the prestressing force is applied through a high-strength steel cable housed within the bottom foot of the cross-section. Channel lips distinguish the geometry of the cross-section with two longitudinal stiffeners in the trunk and two openings in the bottom flange through which the cable passes. Due to the eccentric position of the cable with respect to the strong geometric axis of the member, the prestressing force introduces initial tensile stresses within the upper region of the cold-formed steel beam, thus canceling part of the compressive stresses induced during the subsequent stage of the imposed vertical loading. Consequently, the occurrence of local instabilities is delayed and thus the cold-formed steel member can carry a higher load before failure, i.e. its load-carrying capacity is enhanced. This phenomenon is called prestressing. In addition, the overall vertical deformations of the member are reduced and therefore its functional performance is also improved.

Prestressed cold-formed steel beams are subjected to two loading stages. In Stage I, the prestressing force is transferred to the cold-formed steel member and, in Stage II, a uniformly distributed load is applied along the length of the member. To capture the linear

elastic response of the beams during these two stages, analytical expressions were developed in Chapter 3.

In Chapter 4, the behavior of the cold-formed prestressed beams during the different loading stages, geometrically and materially, was simulated by nonlinear finite element (FE) analysis. In the FE models, shell and truss elements were used to model the steel and cable cross-section respectively, while a fairly fine mesh was used to discretize the member. Two material models were used to model the cold-formed steel member, namely elastic-perfect plastic and two-stage modified Ramberg-Osgood models. The cable was modeled using an elastic-perfect-plastic model.

In Chapter 5, the effect of prestressing on the behavior of the beams under study was studied, making comparisons of the moment-deflection responses and deformed geometries for the bare cold-formed steel beam, the non-prestressed beam with presence of cable and the fully prestressed beam for both linear-elastic material as well as for non-linear. The presence of the prestressed cable played a decisive role in increasing the strength, stiffness of the system as well as in reducing the deformations in the center of the cross-section. The non-linearity of the material resulted in reduced strength of the system. In addition, factors such as the radius of the cable, can significantly increase the strength of the system, but at the risk of increasing the cost of the construction, since more material is used. Finally, the number of openings contributes significantly to the strength of the system since the more openings there are, the less rigid the beam becomes, thus reducing its strength.

6.2 Potential applications in practice

The increase in load-carrying capacity and functional requirements have led pre-stressed cold-formed steel beams to provide highly efficient structural solutions and open up new applications in construction. Of course, the prestressing installation entails higher costs than conventional beams. In addition, the cost of the cable and anchorage should also be taken into account as well. Finally, factors such as durability and maintenance are decisive for the final choice of prestressed systems.

In more detail, the increased structural performance of the proposed beams implies that, for a given capacity and span length requirement, a smaller cold-formed steel cross-section is required, hence material and cost savings, compared to conventional non-prestressed beams. This may allow using the proposed concept in composite flooring systems with thin slabs.

Potentially, the proposed beams can also be used as primary structural elements in the construction of buildings and other structures. For this purpose, the beams can be placed in a back-to-back arrangement to enhance the lateral stability of the prestressed system and avoid asymmetries in the cross-section. Potentially, in this configuration, the addition of prestressed cables may provide even greater improvements in the moment capacity of the cold-formed steel members.

6.3 Further research

This chapter aims to encourage and provide recommendations for further research on the proposed concept.

Prestressed cold-formed steel beams can be placed in a back-to-back arrangement to enhance the load-bearing capacity and improve the lateral stability of the member. A pilot study on the behavior of cold-formed steel prestressed beams has been carried out by Hadjipantelis et al. (2018). They concluded that it can provide benefits of up to 60% in the moment capacity of the beams and reductions of close to 70% in their overall deformations. A study on the benefits of the back-to-back beam arrangement has been carried out by Kanthasamy et al. (2022). Therefore, the combination of these studies i.e. cold formed beams with the presence of pre-stressed cable in a back-to-back arrangement can bring significant improvements in the strength and stiffness of the systems. In addition, the back-to-back cross sections could be compared with the embedded closed cross sections. Extensive research on embedded closed sections was carried out by Li, Q. and Young, B., (2022) where it could be clarified which arrangement offers the most advantages.

In addition, the system of anchoring the cable to the beam is a major issue since it was not studied in this study. By selecting a suitable anchoring system, an optimal transfer of the prestressing force will be achieved without losses and achieving its full utilization. In the present work it was assumed that there are no pretensioning losses.

Finally, another topic of study could be the influence of the cold forming process on the material response, the residual stresses and the initial geometric defects of the beam. Experimental investigations could test different beam geometries and cable sizes.

Bibliography

AISI S100-16, 2016. American Iron and Steel Institute.
Al Ali, M., 2014. Thin-walled cold-formed compressed steel members and the problem of initial imperfections. Advanced Materials Research.
Al Ali, M. and Tomko, M., 2014. Analysis of the Resistance of Thin-Walled Cold-Formed Compressed Steel Members with Closed Cross-sections. Part 2. Magazine of Civil Engineering.
Al Ali, M., Tomko, M., Badak, M., 2013. Analysis of the resistance of thin-walled cold-formed compressed steel members with closed cross-sections. Part 1. Magazine of Civil Engineering.
Casson, L, 1971. Ships and seamanship in the ancient world. Princeton: Princeton University Press.
Clarke, M. J. and Hancock, G. J, 1991. Finite-element nonlinear analysis of stressed arch frames. Journal of Structural Engineering.
CSSBI, 2021. URL https://cssbi.ca/blog/cold-formed-steel-what-where-why
Davison, B. and Owens, G.W., 2012. Steel designers' manual, 7th Edition. ed. Wiley-Blackwell.
Degtyarev, V.V., Degtyareva, N.V., 2016. Finite element modeling of cold-formed steel channels with solid and slotted webs in shear. Thin-Walled Structures.
Dinis, P. B., Camotim, D., and Silvestre, N, 2007. FEM-based analysis of the local-plate/distortional mode interaction in cold-formed steel lipped channel columns. Computers & Structures.
Dischinger, F, 1949. Stahlbrucken im verbundmit stahlebeton druckplatten bei gleichzeitiger vorspannung durch hochwertige seite (in German). Der Bavingerniever.
EN-1992-1-1, 2004.
EN-1993-1-3, 2006.
Gardner, L. and Ashraf, M., 2006. Structural design for non-linear metallic materials. Engineering Structures.
Gardner, L. and Yun X., 2018. Description of stress-strain curves for cold-formed steels. Construction and Building Materials.
Gosaye, J., Gardner, L., Wadee, M. A., and Ellen, M. E., 2016. Compressive behaviour and design of prestressed steel elements. Structures.
Gosaye, J., Gardner, L., Wadee, M. A., and Ellen, M. E, 2014. Tensile performance of prestressed steel elements. Engineering Structures.
Hadjipantelis, N., Gardner, L., Wadee, M. Ahmer, 2018. Prestressed cold-formed steel beams: Concept and mechanical behaviour.
Haidarali, M. R. and Nethercot, D. A., 2011. Finite element modelling of cold-formed steel beams under local buckling or combined local/distortional buckling. Thin-Walled Structures.
Hancock G.J., 2016. Cold-formed steel structures: Research review 2013-2014. Advances in Structural Engineering.
Hoadley, P. G., 1961. An analytical study of the behavior of prestressed steel beams (Illinois). University of Illinois Urbana-Champaign.
Hoadley, P.G., 1968. Development and use of prestressed steel flexural members: Part 2 - Prestressing by means of high strength steel wires or bars. Journal of the Structural Division.
Hoadley, P.G., 1967. The Nature of Prestressed Steel Structures. Highway Research Record.
Johnson, J, Bryan, C and Turneaure, F, 1894. The theory and practice of modern framed structures, Third edition. ed. New York: John Wiley & Sons.

Kanthasamy, E., Hussain, J., Thirunavukkarasu, K., Pologanathan, K., Roy, K., Ananthi, G.B.G., and Suntharalingam T., 2022. Flexural Behaviour of Built-Up Beams Made of Optimised Sections. Buildings.
Kyvelou, P., Gardner, L., and Nethercot, D.A., 2018. Finite element modelling of composite cold-formed steel flooring systems. Engineering Structures.
Li, Q. and Young, B., 2022. Structural behaviour of cold-formed steel built-up closed section beam–columns. Thin-Walled Structures.
Madrazo-Aguirre, F., Ruiz-Teran, A. M., and Wadee, M. A., 2015a. Dynamic behaviour of steel–concrete composite under-deck cable-stayed bridges under the action of moving loads. Engineering Structures.
Madrazo-Aguirre, F., Wadee, M. A., and Ruiz-Teran, A. M, 2015b. Non-linear stability of under-deck cable-stayed bridge decks. International Journal of Non-Linear Mechanics.
Magnel, G., 1950. Prestressed Steel Structures. The Structural Engineer.
Mirambell, E. and Real, E., 2000. On the calculation of deflections in structural stainless steel beams: an experimental and numerical investigation. Journal of Constructional Steel Research.
Moen, C.D.., 2008. Direct Strength Design of Cold-Formed Steel Members with Perforations. Johns Hopkins University, Baltimore, Maryland.
Moen, C.D. and Schafer, B.W., 2008. Experiments on cold-formed steel columns with openings. Thin-Walled Structures.
Murkowski, W., 1974. Experimental testing of new type of prestressed steel girder. Archives of Civil Engineering.
NAS (North American Specification), 2001.
Natario, P., Silvestre, N., and Camotim, D., 2014. Computational modelling of flange crushing in cold-formed steel sections. Thin-Walled Structures.
Naumes, J., Strohmann, I., Ungermann, D., Sedlacek, G., 2008. Die neuen Stabilitätsnachweise im Stahlbau nach Eurocode 3. Stahlbau.
Osofero, A. I., Wadee, M. A., and Gardner, L., 2012. Experimental study of critical and post-buckling behaviour of prestressed stayed columns. Journal of Constructional Steel Research.
Ramberg, W. and Osgood, W. R., 1943. Description of stress–strain curves by three parameters. National Advisory Committee for Aeronautics.
Ranawaka, T., 2006. Distortional Buckling Behaviour of ColdFormed Steel Compression Members at Elevated Temperatures.
Rasmussen, K. J. R, 2003. Full-range stress–strain curves for stainless steel alloys. Journal of Constructional Steel Research.
Saadatmanesh,H., Albrecht, P., Ayyub,B.M., 1989a. Analytical Study of Prestressed Composite Beams. Structural Engineers.
Saadatmanesh,H., Albrecht, P., Ayyub,B.M., 1989c. Guidelines for Flexural Design of Prestressed Composite Beams. Structural Engineers.
Saito, D. and Wadee, M. A., 2010. Optimal prestressing and configuration of stayed columns. Structures and Buildings. Proceedings of the Institution of Civil Engineers.
Saito, D. and Wadee, M. A., 2008. Post-buckling behaviour of prestressed steel stayed columns. Engineering Structures.
Saito, D. and Wadee, M.A., 2009. Buckling behaviour of prestressed steel stayed columns with imperfections and stress limitation. Engineering Structures.
Schafer, B. W., Li, Z., and Moen, C. D., 2010. Computational modeling of cold-formed steel. Thin-Walled Structures.

Schafer, B.W., 2006. Direct Strength Method design guide. American Iron and Steel Institute (AISI).
Schafer B.W. and Peköz, T., 1998a. Computational modeling of cold-formed steel: characterizing geometric imperfections and residual stresses. Journal of Constructional Steel Research.
Schafer, B.W. and Peköz,T., 1999. Laterally braced cold-formed steel flexural members with edge stiffened flanges. Journal of Structural Engineering.
Standards Australia, 2018.
Stras, J.C., 1964. An experimental and analytical study of prestressed composite beams. Rice University.
Subcommittee 3 on Prestressed Steel of Joint ASCE-AASHO Committee on Steel Flexural Members. Development and use of prestressed steel flexural members., 1968. . Journal of the Structural Division.
Tachibana, Y., Kondo, K., Ito, K, 1964. Experimental study on composite beams prestressed with wire cables. Bridge and Struct. Engineer.
Thompson, J. M. T. and Hunt, G. W., 1973. A general theory of elastic stability. J. Wiley, London.
Tong, W. and Saadatmanesh, H., 1992. Parametric study of continuous prestressed composite girders. Journal of Structural Engineering.
Torabian, S. and Schafer, B. W., 2018. Development and Experimental Validation of theDirect Strength Method for Cold-FormedSteel Beam-Columns. Journal of Structural Engineering.
Torabian, S., Zheng, B., and Schafer, B. W, 2014a. Delopment of a new beam-column design method for cold formed steel lipped channel members. Presented at the 22nd International Specialty Conference on Cold-Formed Steel Structures, St. Louis, Missouri, USA.
Trebilcock P.J., 1994. Building Design Using Cold Formed Steel Sections: An Architect's Guide, SCI P130. ed. Steel Construction Institute.
Troitsky, M. S., Zielinski, Z. A., and Rabbani, N. F, 1989. Prestressed-steel continuous span girders. Journal of Structural Engineering.
Troitsky, M.S., 1990. Prestressed steel bridges: theory and design. Van Nostrand Reinhold Company, New York.
Wadee, M.A., Gardner, L., and Osofero, A.I., 2013. Design of prestressed stayed columns. Journal of Constructional Steel Research.
Wang, J., Afshan, S., and Gardner, L., 2017. Axial behaviour of prestressed high strength steel tubular members. Journal of Constructional Steel Research.
Young, B. and Yan, J., 2004. Numerical investigation of channel columns with complex stiffeners—part II: parametric study and design. Thin-Walled Structures.
Yu, C. and Schafer, B. W., 2007. Simulation of cold-formed steel beams in local and distortional buckling with applications to the direct strength method. Journal of Constructional Steel Research.
Yu, C. and Schafer, B. W, 2006. Distortional buckling tests on cold-formed steel beams. Journal of Structural Engineering.
Yu, C. and Schafer, B.W., 2003. Local Buckling Tests on Cold-formed Steel Beams. Journal of Structural Engineering.
Yu, J. and Wadee, M. A., 2017. Mode interaction in triple-bay prestressed stayed columns. International Journal of Non-Linear Mechanics.
Yun, X. and Gardner, L, 2017. Stress–strain curves for hot-formed steels. Journal of Constructional Steel Research.

Zeinoddini, V.M. and Schafer, B.W., 2012. Simulation of geometric imperfections in cold-formed steel members using spectral representation approach. Thin-Walled Structures.